Scattering of low energy neutrinos and antineutrinos by atomic electrons

Ian B. Whittingham

College of Science and Engineering, James Cook University, Townsville, Queensland 4811, Australia

(Received 28 September 2021; accepted 9 December 2021; published 12 January 2022)

Studies of neutrino mixing and oscillations, solar neutrinos as background in dark matter searches involving electron detection, detection of sterile neutrino warm dark matter, and of possible electromagnetic properties of neutrinos, have generated interest in the low energy O(10 keV) scattering of electron neutrinos and antineutrinos by atomic electrons where the binding of the atomic electron cannot be ignored. Of particular interest is the ionization of atoms by neutrinos and antineutrinos. Most existing calculations are based upon modifications of the free electron differential cross section which destroy the relationship between the neutrino helicities and the orbital and spin angular momenta of the atomic electrons. The present calculations maintain the full collision dynamics by formulating the scattering in configuration space using the bound interaction picture, rather than the usual formulation in the interaction picture in momentum space as appropriate to scattering by free electrons. Energy spectra of ionization electrons produced by scattering of neutrinos and antineutrinos with energies of 5, 10, 20, and 30 keV by hydrogen, helium and neon have been calculated using Dirac central field eigenfunctions, and are presented as ratios to the spectra for scattering by free electrons. Binding effects increase strongly with atomic number, are largest for low neutrino energy and, for each neutrino energy, greatest at the high electron energy end of the spectrum. The most extreme effects of binding are for 5 keV scattering by Ne where the ratios are less than 0.1. The energy spectra have been calculated for both a Coulombic final electron state and a free final electron state. The results indicate that the binding effects from the continuum state of the final electron are significant and can be comparable to those arising from the bound initial electron state.

DOI: 10.1103/PhysRevD.105.013008

I. INTRODUCTION

Studies of neutrino mixing and oscillations [1], solar neutrinos as background in dark matter searches involving electron detection [2], detection of sterile neutrino warm dark matter [3], and of possible electromagnetic properties of neutrinos, such as magnetic and electric dipole moments, using low energy elastic scattering of neutrinos and antineutrinos [4,5], have generated interest in the low energy O(10 keV) scattering of electron neutrinos and antineutrinos by atomic electrons

$$\nu_e(\bar{\nu}_e) + e^- \rightarrow \nu_e(\bar{\nu}_e) + e^-. \tag{1}$$

The standard scattering is due to the weak interaction and involves both W-boson charged current and Z-boson neutral current exchange. If neutrinos do have electromagnetic properties, generated by quantum loop effects, there will also be scattering due to single photon exchange. The weak and electromagnetic scatterings are incoherent and their dependences upon the energy transferred $T = E_{\nu_i} - E_{\nu_f}$ to the atomic electron for $T \ll E_{\nu_i}$ are quite different, with their differential cross sections $d\sigma/dT$ being approximately constant for the standard scattering and $\propto 1/T$ for the electromagnetic scattering. The effect of a neutrino magnetic moment is then a distortion in the shape of the atomic electron recoil spectrum at low E_{ν_i}. For all these low energy studies the binding of the atomic electron cannot be ignored and one can expect modifications of the free electron scattering formulas. Neutrino-atom collisions has been reviewed by Kouzakov and Studenikin [6]. In this present study we consider only the scattering by the standard weak interaction.

Of particular interest is the ionization of atoms by neutrinos and antineutrinos. The case of ionization of hydrogen-like atoms was first considered by [7] who found the ionization cross section per electron exceeded the free electron cross section by a factor of 2 or 3 for neutrino energies $E_\nu \sim \alpha Z m_e$. Subsequently, calculated electron spectra from inelastic scattering of neutrinos by atomic electrons of ^{19}F and ^{96}Mo were found [8,9] to differ significantly from scattering by a free electron and were always smaller than the

free electron case. Ionization cross sections for scattering by bound electrons in the light atoms H, He and Ne were also found [10] to be smaller than the corresponding free electron cross sections. The calculations were then extended [11] to the electron spectra for H, He and Ne, and integrated ionization cross sections for H, He, Ne and Xe.

The calculations of [10,11] are based upon the assumption of spin-independent nonrelativistic atomic wave functions and consider the scattering to occur from a free electron whose energy E_{e_i} is set to the energy of the initial bound electron $m_e + \epsilon$, where ϵ is the binding energy, and whose momentum $\mathbf{p}_{e_i}$ is determined by the probability amplitude $|\Psi_{n_i l_i m_i}(\mathbf{p}_{e_i})|^2$, where $\Psi_{n_i l_i m_i}(\mathbf{p}_{e_i})$ is the momentum-space atomic wave function. The bound electron is then described by the effective squared mass

$$\tilde{m}^2 = p_{e_i}^2 = E_{e_i}^2 - \mathbf{p}_{e_i}^2. \tag{2}$$

Coulombic effects on the final electron are also ignored. This allows the ν_e-electron scattering process to be described as a probability weighted scattering by a free electron of mass $\tilde{m}$. This scattering can then be averaged (summed) over all initial (final) electron and neutrino spin states, giving the invariant squared scattering amplitude

$$\begin{aligned}|F(\nu_e e^- \to \nu_e e^-)|^2 = 2G_F^2\{&(\bar{v}_e - \bar{a}_e)^2(s - m_e^2)(s - \tilde{m}^2) \\ &+ (\bar{v}_e + \bar{a}_e)^2(u - m_e^2)(u - \tilde{m}^2) \\ &+ 2m_e^2(\bar{v}_e^2 - \bar{a}_e^2)t\},\end{aligned} \tag{3}$$

where

$$s = (p_{\nu_i} + p_{e_i})^2, \quad t = (p_{\nu_i} - p_{\nu_f})^2, \quad u = (p_{\nu_i} - p_{e_f})^2, \tag{4}$$

are the usual kinematic invariants, and it has been assumed that the scattering occurs at low momentum transfers $t^2 \ll M_{Z,W}^2$. Here, $\bar{v}_e = 1 + 4\sin^2\theta_W$ and $\bar{a}_e = -1$ where θ_W is the weak mixing angle. For scattering by a free electron, $\tilde{m}^2$ is replaced by m_e^2. The result for $\overline{\nu_e}$-electron scattering follows from (3) by interchanging s and u. The differential cross section in this approach is

$$\begin{aligned}d\sigma = &\frac{1}{16\pi^2 E_{\nu_i} E_{e_i}} \delta^{(4)}(p_{e_f} + p_{\nu_f} - p_{e_i} - p_{\nu_i}) \\ &\times |\Psi_{n_i l_i m_i}(\mathbf{p}_{e_i})|^2 \frac{d^3\mathbf{p}_{e_i}}{(2\pi)^3} \\ &\times |F(\nu_e e^- \to \nu_e e^-)|^2 \frac{d^3\mathbf{p}_{\nu_f}}{2E_{\nu_f}} \frac{d^3\mathbf{p}_{e_f}}{2E_{e_f}}.\end{aligned} \tag{5}$$

An alternative approach has been introduced [12–14] which assumes $T \ll E_{\nu_i}$ and $T \ll m_e$ so that the electrons and scattering can be treated non-relativistically. The atomic target is considered to be unpolarized. The differential cross section is then the low-T form of the free electron result modified to the form

$$\frac{d\sigma}{dT} = \frac{G_F^2}{4\pi}(1 + 4\sin^2\theta_W + 8\sin^4\theta_W) \int S(T, q^2) dq^2, \tag{6}$$

where $S(T, q^2)$ is the dynamical structure function

$$S(T, q^2) = \sum_f \delta(T - E_f + E_i) |\langle f|\rho(\mathbf{q})|i\rangle|^2, \tag{7}$$

and $\mathbf{q}$ is the spatial momentum transfer with $T^2 \le q^2 \le 4E_{\nu_i}^2$. The sum is over all final atomic states $|f\rangle$ of energy E_f consistent with energy conservation, with $|i\rangle$ being the initial state. Here

$$\rho(\mathbf{q}) = \sum_{a=1}^{Z} \exp(i\mathbf{q} \cdot \mathbf{r}_a) \tag{8}$$

is the Fourier transform of the electron number density and the sum is over the positions $\mathbf{r}_a$ of all the Z electrons in the atom.

The dynamical structure function is evaluated through its relationship

$$S(T, q^2) = \frac{1}{\pi} \mathrm{Im} F(T, q^2). \tag{9}$$

to the density-density Green's function

$$F(T, q^2) = \sum_f \frac{|\langle f|\rho(\mathbf{q})|i\rangle|^2}{T - E_f + E_i - i\epsilon}. \tag{10}$$

Atomic binding deforms the density-density Green's function by broadening and shifting the free electron δ-peak at $q^2 = 2m_e T$, but Kouzakov *et al* [14] argue that the modifications relative to the free-electron expressions are quite small. Analytical results are obtained for $1s$, $2s$ and $2p$ hydrogenlike states.

The more recent calculations by Chen *et al.* [15–17] use the four-fermion contact form for the weak interaction

$$\frac{d^2\sigma}{dT d\Omega} = \frac{G_F^2}{2\pi^2} \frac{E_{\nu_f}}{E_{\nu_i}} L^{(\nu)\alpha\beta} R_{\alpha\beta}^{(w)} \tag{11}$$

where the scattering of the neutrino of momentum p_{ν_i} and helicity s_i is described by the tensor

$$\begin{aligned}L^{(\nu)\alpha\beta} = &\langle p_{\nu_f}, s_f|\gamma^\alpha(1 - \gamma_5)|p_{\nu_i}, s_i\rangle \\ &\times \langle p_{\nu_f}, s_f|\gamma^\beta(1 - \gamma_5)|p_{\nu_i}, s_i\rangle^*.\end{aligned} \tag{12}$$

The effects on the atomic system are represented by the response functions

$$R^{(w)}_{\alpha\beta} = \frac{1}{2j_i+1}\sum_{m_{j_i}}\sum_f \langle f|j^\alpha_w|i\rangle\langle f|j^\beta_w|i\rangle^* \times \delta(T+E_i-E_f), \quad (13)$$

which involve a sum/integral over the final atomic electron states $|f\rangle$ and a spin average over the initial atomic states $|i\rangle = |j_i, m_{j_i}, \ldots\rangle$. The relativistic weak current representing the sum of the charged and neutral currents is

$$j^\alpha_w = \frac{1}{2}\overline{e}'(\bar{v}_e\gamma^\alpha + \bar{a}_e\gamma^\alpha\gamma_5)e. \quad (14)$$

The model has been applied to Ge with the response functions evaluated using the multiconfiguration relativistic random phase approximation. Consequently, the leading relativistic terms in the atomic Hamiltonian are treated nonperturbatively by using Dirac eigenfunctions, the two possible configurations for the Ge ground state are included, and the Random Phase Approximation accounts for the two-body correlations. The weak current operator (14) is expanded in spherical multipoles.

The calculations [10–14] destroy the relationship between the neutrino helicities and the orbital and spin angular momenta of the atomic electrons. Some of these issues are addressed by [16,17], and their approach is closest in spirit to the present calculations. To maintain the full collision dynamics, the scattering of the neutrino by the bound electron will be treated in a similar manner to that of bound Compton scattering [18] in that the scattering will be formulated in configuration space using the Furry bound interaction picture [19] rather than the usual formulation in the interaction picture in momentum space as appropriate to scattering by free electrons.

The general formalism for the scattering of neutrinos and antineutrinos by atomic electrons is presented in Sec. II. This includes the derivation of the S-matrix and differential cross sections for the scattering processes in terms of the contraction of neutrino and atomic electron tensor amplitudes, and the explicit evaluation of the atomic electron amplitude for the case of an atomic electron represented by a central field Dirac eigenfunction. The nature of the radial matrix elements which occur in the atomic electron amplitude are discussed in Sec. III, and issues relating to the evaluation of the cross sections in Sec. IV. Results for the energy spectra of the ionization electrons produced by scattering of neutrinos and antineutrinos off hydrogen, helium and neon are presented and discussed in Sec. V. Section VI contains a summary and conclusions for the investigation. Details of the derivation of the S-matrix in the Bound Interaction Picture are given in Appendix A, explicit expressions for the electron scattering tensors in Appendix B, and computational details for the evaluation of the radial matrix elements in Appendix C.

II. GENERAL FORMALISM

A. S-matrix for scattering by bound electrons

As discussed above, in order to treat the effects of atomic binding on the scattering of neutrinos by atomic electrons, the second-order S-matrix element will be developed in the Furry picture [19] in which the electron is in the presence of a c-number electromagnetic field $A^{(\mathrm{ext})}_\alpha(x)$ and the electron field operator satisfies

$$[i\gamma^\alpha\partial_\alpha - e\gamma^\alpha A^{(\mathrm{ext})}_\alpha(x) - m_e]e(x) = 0, \quad (15)$$

where $\partial_\alpha \equiv \partial/\partial x^\alpha$. The natural unit system $\hbar = c = 1$ is used throughout, the scalar product of two 4-vectors is $A\cdot B \equiv g^{\alpha\beta}A_\alpha B_\beta = A_0B_0 - \mathbf{A}\cdot\mathbf{B}$, the Dirac matrices γ^α, $(\alpha = 0, 1, 2, 3)$ satisfy $\{\gamma^\alpha, \gamma^\beta\} = 2g^{\alpha\beta}$, $\gamma_5 \equiv i\gamma^0\gamma^1\gamma^2\gamma^3$, and the field operators for a given particle are denoted by the symbol for that particle.

The part of the Standard Model lepton interaction Lagrangian which describes the interactions between an electron-neutrino ν_e and an electron e is [20,21]

$$\mathcal{L}^{\nu_e e}_I = \mathcal{L}^{\nu_e We}_I + \mathcal{L}^{\nu_e Z\nu_e}_I + \mathcal{L}^{eZe}_I, \quad (16)$$

where

$$\mathcal{L}^{\nu_e We}_I = \frac{-g}{2\sqrt{2}}N[\overline{\nu_e}\gamma^\alpha(1-\gamma_5)W^{(+)}_\alpha e + \overline{e}\gamma^\alpha(1-\gamma_5)W^{(-)}_\alpha\nu_e], \quad (17)$$

$$\mathcal{L}^{\nu_e Z\nu_e}_I = \frac{-g}{4\cos\theta_W}N[\overline{\nu_e}\gamma^\alpha(1-\gamma_5)Z_\alpha\nu_e], \quad (18)$$

$$\mathcal{L}^{eZe}_I = \frac{-g}{4\cos\theta_W}N[\overline{e}\gamma^\alpha(v_e + a_e\gamma_5)Z_\alpha e]. \quad (19)$$

Here g is the $SU(2)$ gauge coupling constant, $v_e = -1 + 4\sin^2\theta_W$ and $a_e = 1$ are the weak neutral current parameters, $W^{(\pm)}$ and Z are the charged and neutral weak gauge boson field operators respectively, and N is the normal ordering operator.

The total S-matrix for ν_e scattering at low momentum transfers $k^2 \ll M_A^2$, where $A = W, Z$, is (see Appendix A)

$$S^{(\nu)}_{fi} = -\pi i\frac{G_\mathrm{F}}{\sqrt{2}}\delta(E^{(\nu)}_{fi})M^{(e)}_{n_f,n_i}(\mathbf{q})^\alpha M^{(\nu)}(\mathbf{p}_{\nu_f}, s_f, \mathbf{p}_{\nu_i}, s_i)_\alpha \quad (20)$$

where

$$M^{(e)}_{n_f,n_i}(\mathbf{q})^\alpha = \int d^3x e^{i(\mathbf{p}_{\nu_i}-\mathbf{p}_{\nu_f})\cdot\mathbf{x}} \times \bar{\phi}^{(+)}_{n_f}(\mathbf{x})\gamma^\alpha(\bar{v}_e + \bar{a}_e\gamma_5)\phi^{(+)}_{n_i}(\mathbf{x}), \quad (21)$$

and

$$M^{(\nu)}(\mathbf{p}_{\nu_f}, s_f, \mathbf{p}_{\nu_i}, s_i)_\alpha = \bar{u}^{(s_f)}(\mathbf{p}_{\nu_f})\gamma_\alpha(1-\gamma_5)u^{(s_i)}(\mathbf{p}_{\nu_i}). \quad (22)$$

Here $u^{(s)}(\mathbf{p}_\nu)$ are the plane wave spinors describing a neutrino with momentum $\mathbf{p}_\nu$ and helicity s, and $\phi_n^{(+)}(\mathbf{x})$ is the energy eigenfunction for an electron in a state of the external field $A^{(\mathrm{ext})}$ specified by the quantum numbers n. The quantity

$$\delta(E_{fi}^{(\nu)}) \equiv \delta(E_{n_f} + E_{\nu_f} - E_{n_i} - E_{\nu_i}). \quad (23)$$

incorporates energy conservation, and $\mathbf{q} = \mathbf{p}_{\nu_i} - \mathbf{p}_{\nu_f}$ is the momentum transfer from the neutrino. The electron mixing parameters are

$$\bar{v}_e = v_e + 2 = 1 + 4\sin^2\theta_W, \quad \bar{a}_e = a_e - 2 = -1. \quad (24)$$

For scattering of antineutrinos, $M^{(\nu)}$ is replaced by

$$M^{(\bar{\nu})}(\mathbf{p}_{\nu_f}, s_f, \mathbf{p}_{\nu_i}, s_i)_\alpha = \bar{v}^{(s_i)}(\mathbf{p}_{\nu_i})\gamma_\alpha(1-\gamma_5)v^{(s_f)}(\mathbf{p}_{\nu_f}), \quad (25)$$

where $v^{(s)}(\mathbf{p}_\nu)$ is the antineutrino plane wave spinor, and $\delta(E_{fi}^{(\nu)})$ is replaced by $\delta(E_{fi}^{(\bar{\nu})})$.

B. Cross section

We assume each atomic electron acts as an independent scattering center. In order to obtain the scattering cross section per atomic electron, $S_{fi}^{(\nu)}$ is expressed in the form

$$S_{fi}^{(\nu)} = \delta(E_{n_f} + E_{\nu_f} - E_{n_i} - E_{\nu_i})\mathcal{M}_{fi}^{(\nu)}. \quad (26)$$

The corresponding transition probability per unit time is then [22]

$$dP_{fi}^{(\nu)} = \frac{1}{2\pi}\delta(E_{n_f} + E_{\nu_f} - E_{n_i} - E_{\nu_i})|\mathcal{M}_{fi}^{(\nu)}|^2. \quad (27)$$

For ν_e scattering into the momentum interval $(\mathbf{p}_{\nu_f}, \mathbf{p}_{\nu_f} + d^3\mathbf{p}_{\nu_f})$, the transition probability per unit time is

$$dP^{(\nu)} = \sum_{n_f} dP_{fi}^{(\nu)} d\rho_f^{(\nu)} d\rho_f^{(e)}, \quad (28)$$

where $d\rho_f^{(\nu)}$ ($d\rho_f^{(e)}$) is the density of final ν_e (e) states and the sum is over all final electron states consistent with energy conservation. For plane wave neutrino spinors normalized to $u^{\dagger(s)}(\mathbf{p}_\nu)u^{(s)}(\mathbf{p}_\nu) = 2E_\nu$, the density of states is $d\rho_f^{(\nu)} = d^3\mathbf{p}_{\nu_f}/[(2\pi)^3 2E_{\nu_f}]$ and the incident neutrino flux is $2E_{\nu_i}$.

The differential cross section is then

$$d\sigma^{(\nu)} = \frac{dP^{(\nu)}}{2E_{\nu_i}} = \frac{1}{2E_{\nu_i}}\sum_{n_f} dP_{fi}^{(\nu)} \frac{d^3\mathbf{p}_{\nu_f}}{(2\pi)^3 2E_{\nu_f}} d\rho_f^{(e)}. \quad (29)$$

Writing $d^3\mathbf{p}_{\nu_f} = E_{\nu_f}^2 dE_{\nu_f} d\Omega_{\nu_f}$ then

$$d\sigma^{(\nu)} = \frac{1}{(2\pi)^4}\frac{1}{4E_{\nu_i}}\sum_{n_f}\delta(E_{fi}^{(\nu)}) \times E_{\nu_f} dE_{\nu_f} d\Omega_{\nu_f} d\rho_f^{(e)} |\mathcal{M}_{fi}^{(\nu)}|^2, \quad (30)$$

where, from (20),

$$\mathcal{M}_{fi}^{(\nu)} = -\pi i \frac{G_\mathrm{F}}{\sqrt{2}} M_{n_f,n_i}^{(e)}(\mathbf{q})^\alpha M^{(\nu)}(\mathbf{p}_{\nu_f}, s_f, \mathbf{p}_{\nu_i}, s_i)_\alpha. \quad (31)$$

The neutrino contribution to $|\mathcal{M}_{fi}^{(\nu)}|^2$ is [21]

$$\begin{aligned} L^{(\nu)}(p_{\nu_i}, p_{\nu_f})^{\beta\alpha} &\equiv [\bar{u}^{(s_f)}(\mathbf{p}_{\nu_f})\gamma^\beta(1-\gamma_5)u^{(s_i)}(\mathbf{p}_{\nu_i})]^\dagger \\ &\quad \times \bar{u}^{(s_f)}(\mathbf{p}_{\nu_f})\gamma^\alpha(1-\gamma_5)u^{(s_i)}(\mathbf{p}_{\nu_i}) \\ &= 8(p_{\nu_i}^\beta p_{\nu_f}^\alpha + p_{\nu_i}^\alpha p_{\nu_f}^\beta - p_{\nu_i}\cdot p_{\nu_f} g^{\beta\alpha} \\ &\quad + i\epsilon^{\rho\beta\lambda\alpha} p_{\nu_i,\rho} p_{\nu_f,\lambda}), \end{aligned} \quad (32)$$

where $s_i = s_f = -1/2$. The scattering of antineutrinos involves

$$\begin{aligned} L^{(\bar{\nu})}(p_{\nu_i}, p_{\nu_f})^{\beta\alpha} &\equiv [\bar{v}^{(s_i)}(\mathbf{p}_{\nu_i})\gamma^\beta(1-\gamma_5)v^{(s_f)}(\mathbf{p}_{\nu_f})]^\dagger \\ &\quad \times \bar{v}^{(s_i)}(\mathbf{p}_{\nu_i})\gamma^\alpha(1-\gamma_5)v^{(s_f)}(\mathbf{p}_{\nu_f}) \\ &= L^{(\nu)}(-p_{\nu_f}, -p_{\nu_i})^{\beta\alpha}, \\ &= [L^{(\nu)}(p_{\nu_i}, p_{\nu_f})^{\beta\alpha}]^*, \end{aligned} \quad (33)$$

where $s_i = s_f = +1/2$.

C. Atomic electron amplitude

The electron amplitude (21) requires the solutions $\phi_n^{(+)}(x)$ of (15). We assume the atomic electron moves in a spherically symmetric potential $V(r) = eA^{(\mathrm{ext})}(r)$ and use the Dirac representation for the γ matrices

$$\gamma^0 = \begin{pmatrix} I & 0 \\ 0 & -I \end{pmatrix}, \quad \gamma^k = \begin{pmatrix} 0 & \sigma^k \\ -\sigma^k & 0 \end{pmatrix}, \quad \gamma_5 = \begin{pmatrix} 0 & I \\ I & 0 \end{pmatrix}, \quad (34)$$

where σ^k, $k = 1, 2, 3$, are the Pauli 2×2 matrices, and I is the unit 2×2 matrix. The eigenfunctions have the form [23]

$$\phi_{\kappa,\mu,E}(r,\theta,\varphi) = \frac{1}{r}\begin{pmatrix} g_{\kappa,E}(r)\chi_\kappa^\mu(\Omega) \\ i f_{\kappa,E}(r)\chi_{-\kappa}^\mu(\Omega) \end{pmatrix}. \quad (35)$$

where $(r,\theta,\varphi) = (r,\Omega)$ are spherical polar coordinates, and $\chi_\kappa^\mu(\Omega)$ are the spinor spherical harmonics

$$\chi_\kappa^\mu(\Omega) = \sum_{m_s} C\left(l_\kappa, \frac{1}{2}, j, \mu - m_s, m_s, \mu\right) Y_{l_\kappa}^{\mu-m_s}(\Omega)\chi_{m_s}. \quad (36)$$

Here $C(j_1, j_2, j_3, m_1, m_2, m_3)$ is a Clebsch-Gordon coefficient, and χ_{m_s} are the two component Pauli spinors. The total angular momentum j and orbital angular momentum l_κ are obtained from the quantum number κ by

$$j = |\kappa| - \frac{1}{2}, \quad l_\kappa = \begin{cases} \kappa & \kappa > 0 \\ -\kappa - 1 & \kappa < 0 \end{cases}, \quad l_{-\kappa} = l_\kappa - \frac{\kappa}{|\kappa|}, \quad (37)$$

where κ takes all nonzero integral values. Note that the subscript e has been dropped from the electron energies. The radial functions satisfy

$$\begin{pmatrix} d/dr + \kappa/r & -(E + m_e - V(r)) \\ E - m_e - V(r) & d/dr - \kappa/r \end{pmatrix} \begin{pmatrix} g_{\kappa,E}(r) \\ f_{\kappa,E}(r) \end{pmatrix} = 0. \quad (38)$$

As no observation is made upon the final continuum electron, all possible states of the electron must be summed over, with the result that the asymptotic form of the continuum eigenfunction is not important [24]. Any set of continuum functions may be used and the form (35) is the obvious choice.

In order to evaluate

$$N^\alpha_{fi}(\mathbf{q}) \equiv \int r^2 dr d\Omega e^{i\mathbf{q}\cdot\mathbf{r}} \bar{\phi}_{\kappa_f,\mu_f,E_f}(r,\theta,\varphi) \times \gamma^\alpha(\bar{v}_e + \bar{a}_e\gamma_5)\phi_{\kappa_i,\mu_i,E_i}(r,\theta,\varphi), \quad (39)$$

we introduce the expansion

$$e^{i\mathbf{q}\cdot\mathbf{r}} = 4\pi \sum_{l=0}^{\infty} \sum_{m=-l}^{+l} i^l j_l(|\mathbf{q}|r) Y^m_l(\hat{\mathbf{q}})^* Y^m_l(\Omega) \quad (40)$$

and note that

$$\Gamma^{(\alpha)} \equiv \gamma^0\gamma^\alpha(\bar{v}_e + \bar{a}_e\gamma_5) \quad (41)$$

have the form

$$\Gamma^{(0)} = \begin{pmatrix} \bar{v}_e & \bar{a}_e \\ \bar{a}_e & \bar{v}_e \end{pmatrix}, \quad (42)$$

$$\Gamma^{(k)} = \begin{pmatrix} \bar{a}_e\sigma^k & \bar{v}_e\sigma^k \\ \bar{v}_e\sigma^k & \bar{a}_e\sigma^k \end{pmatrix}. \quad (43)$$

Hence (39) becomes

$$N^{(0,k)}_{fi}(\mathbf{q}) = 4\pi \sum_{l,m} i^l Y^m_l(\hat{\mathbf{q}})^* \times \{[\bar{v}_e(\bar{a}_e)[I^{gg}_l(q)\langle\chi^{\mu_f}_{\kappa_f}|Y^m_l(I,\sigma^k)|\chi^{\mu_i}_{\kappa_i}\rangle + I^{ff}_l(q)\langle\chi^{\mu_f}_{-\kappa_f}|Y^m_l(I,\sigma^k)|\chi^{\mu_i}_{-\kappa_i}\rangle]] + i\bar{a}_e(\bar{v}_e)[I^{gf}_l(q)\langle\chi^{\mu_f}_{\kappa_f}|Y^m_l(I,\sigma^k)|\chi^{\mu_i}_{-\kappa_i}\rangle - I^{fg}_l(q)\langle\chi^{\mu_f}_{-\kappa_f}|Y^m_l(I,\sigma^k)|\chi^{\mu_i}_{\kappa_i}\rangle]\} \quad (44)$$

where, e.g., $\bar{v}_e(\bar{a}_e)$ for $\alpha = 0(k)$ respectively, $q \equiv |\mathbf{q}|$ and the radial integrals are

$$I^{gg}_l(q) \equiv \int dr\, g^*_{\kappa_f,E_f}(r) j_l(qr) g_{\kappa_i,E_i}(r),$$
$$I^{gf}_l(q) \equiv \int dr\, g^*_{\kappa_f,E_f}(r) j_l(qr) f_{\kappa_i,E_i}(r),$$
$$I^{fg}_l(q) \equiv \int dr\, f^*_{\kappa_f,E_f}(r) j_l(qr) g_{\kappa_i,E_i}(r),$$
$$I^{ff}_l(q) \equiv \int dr\, f^*_{\kappa_f,E_f}(r) j_l(qr) f_{\kappa_i,E_i}(r). \quad (45)$$

Here on we use the simplified notation $l_{\kappa_{i,f}} = l_{i,f}$, $l_{-\kappa_{i,f}} = l'_{i,f}$ and $m_{s_{i,f}} = m_{i,f}$.

The matrix elements of σ^k can be evaluated by transforming to a spherical basis $\sigma^\lambda, \lambda = 0, \pm 1$, where

$$\sigma^{\pm 1} \equiv \mp \frac{1}{\sqrt{2}}(\sigma^1 \pm i\sigma^2), \qquad \sigma^0 = \sigma^3 \quad (46)$$

and using the Wigner-Eckart theorem

$$\langle\chi_{m_f}|\sigma^\lambda|\chi_{m_i}\rangle = C\left(\frac{1}{2}, 1, \frac{1}{2}, m_i, \lambda, m_f\right)\left\langle\frac{1}{2}\middle\|\sigma\middle\|\frac{1}{2}\right\rangle, \quad (47)$$

where the reduced matrix element is

$$\left\langle\frac{1}{2}\middle\|\sigma\middle\|\frac{1}{2}\right\rangle = \sqrt{3}. \quad (48)$$

Similarly,

$$\langle Y^{\mu_f - m_f}_{l_f}|Y^m_l|Y^{\mu_i - m_i}_{l_i}\rangle = C(l_i, l, l_f, \mu_i - m_i, m, \mu_f - m_f) \times \langle l_f||Y_l||l_i\rangle, \quad (49)$$

where

$$\langle l_f||Y_l||l_i\rangle = \frac{[l_i l]}{\sqrt{4\pi}[l_f]} C(l_i, l, l_f, 0, 0, 0). \quad (50)$$

Here $[ab\ldots] = [(2a+1)(2b+1)\ldots]^{1/2}$. The matrix elements between the spinor harmonics in the spherical basis can then be written

$$\langle \chi_{\kappa_f}^{\mu_f} | Y_l^m(\boldsymbol{I}, \sigma^\lambda) | \chi_{\kappa_i}^{\mu_i} \rangle = \frac{[l]}{\sqrt{4\pi}} J_{l,m}^{(I,\lambda)}(\kappa_f, \kappa_i) \tag{51}$$

where

$$\begin{aligned} J_{l,m}^{(I)}(\kappa_f, \kappa_i) &= \frac{[l_i]}{[l_f]} C(l_i, l, l_f, 0, 0, 0) \sum_{m_f, m_i} C\left(l_f, \frac{1}{2}, j_f, \mu_f - m_f, m_f, \mu_f\right) C\left(l_i, \frac{1}{2}, j_i, \mu_i - m_i, m_i, \mu_i\right) \\ &\quad \times C(l_i, l, l_f, \mu_i - m_i, m, \mu_f - m_f) \delta_{m_f, m_i} \delta_{m, \mu_f - \mu_i} \\ &= \delta_{m, \mu_f - \mu_i} [l_i j_i] C(l_i, l, l_f, 0, 0, 0) W\left(l, l_i, j_f, \frac{1}{2}, l_f, j_i\right) C(l, j_i, j_f, \mu_f - \mu_i, \mu_i, \mu_f), \end{aligned} \tag{52}$$

and [18]

$$\begin{aligned} J_{l,m}^{(\lambda)}(\kappa_f, \kappa_i) &= \sqrt{3} \frac{[l_i]}{[l_f]} C(l_i, l, l_f, 0, 0, 0) \sum_{m_f, m_i} C\left(l_f, \frac{1}{2}, j_f, \mu_f - m_f, m_f, \mu_f\right) C\left(l_i, \frac{1}{2}, j_i, \mu_i - m_i, m_i, \mu_i\right) \\ &\quad \times C(l_i, l, l_f, \mu_i - m_i, m, \mu_f - m_f) C\left(\frac{1}{2}, 1, \frac{1}{2}, m_i, \lambda, m_f\right) \\ &= \delta_{m, \mu_f - \mu_i - \lambda} \sqrt{6} [l_i j_i] C(l_i, l, l_f, 0, 0, 0) \sum_f [f] W\left(l, l_i, j_f, \frac{1}{2}, l_f, f\right) W\left(1, \frac{1}{2}, f, l_i, \frac{1}{2}, j_i\right) \\ &\quad \times C(l, f, j_f, \mu_f - \mu_i - \lambda, \mu_i + \lambda, \mu_f) C(j_i, 1, f, \mu_i, \lambda, \mu_i + \lambda), \end{aligned} \tag{53}$$

where $W(a, b, c, d, e, f)$ is a Racah coefficient. The elements with $-\kappa_i$ or $-\kappa_f$ are obtained from the above through the replacements $l_i \to l_i'$ and $l_f \to l_f'$ respectively.

For scattering by all of the electrons in a specified atomic shell or subshell (labeled by κ_i), with no reference being made to the final state of the atomic electron, the cross section must be summed over all possible initial and final electron states. We therefore need the quantities

$$L_{fi}^{(e)}(\mathbf{q})^{\beta\alpha} = \sum_{\kappa_f, \mu_f, \mu_i} N_{fi}^{\beta}(\mathbf{q})^* N_{fi}^{\alpha}(\mathbf{q}). \tag{54}$$

For the case of H, the μ_i summation over electrons in each shell or subshell is replaced by its average over the K-shell.

The calculation of these coefficients is greatly simplified by choosing the coordinate system such that the neutrino momentum transfer $\mathbf{q}$ is along the Oz axis and $\mathbf{p}_{\nu_i}$ lies in the x–z plane. Thus

$$Y_l^m(\hat{\mathbf{q}}) = \frac{[l]}{(4\pi)^{1/2}} \delta_{m,0}. \tag{55}$$

For $m = \mu_f - \mu_i$ this gives $\mu_f = \mu_i$ whereas, for $m = \mu_f - \mu_i - \lambda$, this gives $\lambda = \mu_f - \mu_i$.

We need the combinations

$$A^{(I,I)}(l_1, l_2, l_3, l_4) = \sum_{\mu_f, \mu_i} J_{\bar{l}, \bar{m}}^{(I)}(\pm\kappa_f, \pm\kappa_i)^* J_{l,m}^{(I)}(\pm\kappa_f, \pm\kappa_i), \tag{56}$$

$$A^{(I,\lambda)}(l_1, l_2, l_3, l_4) = \sum_{\mu_f, \mu_i} J_{\bar{l}, \bar{m}}^{(I)}(\pm\kappa_f, \pm\kappa_i)^* J_{l,m}^{(\lambda)}(\pm\kappa_f, \pm\kappa_i), \tag{57}$$

$$A^{(\lambda,I)}(l_1, l_2, l_3, l_4) = \sum_{\mu_f, \mu_i} J_{\bar{l}, \bar{m}}^{(\lambda)}(\pm\kappa_f, \pm\kappa_i)^* J_{l,m}^{(I)}(\pm\kappa_f, \pm\kappa_i), \tag{58}$$

$$A^{(\lambda',\lambda)}(l_1, l_2, l_3, l_4) = \sum_{\mu_f, \mu_i} J_{\bar{l}, \bar{m}}^{(\lambda')}(\pm\kappa_f, \pm\kappa_i)^* J_{l,m}^{(\lambda)}(\pm\kappa_f, \pm\kappa_i). \tag{59}$$

Here $(l_1, l_2, l_3, l_4) = (l_f, l_i, l_f, l_i)$ for the case $(+\kappa_f, +\kappa_i)$, with the replacements $l_i \to l_i'$ for the case $-\kappa_i$ and $l_f \to l_f'$ for the case $-\kappa_f$. With $m = \bar{m} = 0$, then $\lambda = 0$ in (57), (58) and $\lambda' = \lambda$ in (59).

After some standard Racah algebra manipulations (see, e.g., [25]) we obtain

$$A^{(I,I)}_{\bar{l}l}(l_1,l_2,l_3,l_4)=\delta_{\bar{l},l}[j_f j_i]^2\frac{[l_2 l_4]}{[l]^2}C(l_2,l,l_1,0,0,0)C(l_4,l,l_3,0,0,0)W\left(l,l_2,j_f,\frac{1}{2},l_1,j_i\right)W\left(l,l_4,j_f,\frac{1}{2},l_3,j_i\right), \quad (60)$$

$$A^{(I,\lambda)}_{\bar{l}l}(l_1,l_2,l_3,l_4)=\delta_{\lambda,0}(-1)^{j_i-j_f+l}\sqrt{6}[j_f j_i]^2\frac{[l_2 l_4]}{[l]}C(l_2,\bar{l},l_1,0,0,0)C(l_4,l,l_3,0,0,0)C(\bar{l},1,l,0,0,0)$$
$$\times W\left(\bar{l},l_2,j_f,\frac{1}{2},l_1,j_i\right)\sum_f[f]^2W\left(l,l_4,j_f,\frac{1}{2},l_3,f\right)W\left(1,\frac{1}{2},f,l_4,\frac{1}{2},j_i\right)W(\bar{l},j_i,l,f,j_f,1), \quad (61)$$

$$A^{(\lambda,I)}_{\bar{l}l}(l_1,l_2,l_3,l_4)=A^{(I,\lambda)}_{l\bar{l}}(l_3,l_4,l_1,l_2), \quad (62)$$

$$A^{(\lambda',\lambda)}_{\bar{l}l}(l_1,l_2,l_3,l_4)=\delta_{\lambda',\lambda}(-1)^{j_i-j_f-l+\bar{l}+\lambda}6[j_f j_i]^2[l_2 l_4]C(l_2,\bar{l},l_1,0,0,0)C(l_4,l,l_3,0,0,0)$$
$$\times\sum_g C(\bar{l},l,g,0,0,0)C(1,1,g,-\lambda,\lambda,0)\sum_{\bar{f},f}[\bar{f}f]^2W\left(\bar{l},l_2,j_f,\frac{1}{2},l_1,\bar{f}\right)W\left(l,l_4,j_f,\frac{1}{2},l_3,f\right)$$
$$\times W\left(1,\frac{1}{2},\bar{f},l_2,\frac{1}{2},j_i\right)W\left(1,\frac{1}{2},f,l_4,\frac{1}{2},j_i\right)W\left(\bar{l},\bar{f},l,f,j_f,g\right)W(1,\bar{f},1,f,j_i,g). \quad (63)$$

In order to evaluate the quantities (54) we need the Cartesian components $\tilde{A}^{\beta,\alpha}(l_{1234})$, where

$$\tilde{A}^{0,0}_{\bar{l}l}(l_{1234})=A^{(I,I)}_{\bar{l}l}(l_{1234}),$$
$$\tilde{A}^{1,1}_{\bar{l}l}(l_{1234})=\tilde{A}^{2,2}_{\bar{l}l}(l_{1234})=\frac{1}{2}[A^{(1,1)}_{\bar{l}l}(l_{1234})+A^{(-1,-1)}_{\bar{l}l}(l_{1234})],$$
$$\tilde{A}^{1,2}_{\bar{l}l}(l_{1234})=-\tilde{A}^{2,1}_{\bar{l}l}(l_{1234})=-\frac{i}{2}[A^{(1,1)}_{\bar{l}l}(l_{1234})-A^{(-1,-1)}_{\bar{l}l}(l_{1234})],$$
$$\tilde{A}^{0,3}_{\bar{l}l}(l_{1234})=A^{(I,0)}_{\bar{l}l}(l_{1234}),\qquad \tilde{A}^{3,0}_{\bar{l}l}(l_{1234})=A^{(0,I)}_{\bar{l}l}(l_{1234}),$$
$$\tilde{A}^{3,3}_{\bar{l}l}(l_{1234})=A^{(0,0)}_{\bar{l}l}(l_{1234}). \quad (64)$$

For brevity, we have introduced $l_{1234}=\{l_1,l_2,l_3,l_4\}$. Thus we finally obtain

$$L^{(e)}_{fi}(\tilde{\mathbf{q}})^{\beta\alpha}=\sum_{\kappa_f,\bar{l},l}i^{l-\bar{l}}[\bar{l}l]^2[\bar{v}_e^2L^{\beta\alpha}_{v_e v_e}+\bar{a}_e^2L^{\beta\alpha}_{a_e a_e}+\bar{v}_e\bar{a}_e(L^{\beta\alpha}_{v_e a_e}+L^{\beta\alpha}_{a_e v_e})], \quad (65)$$

where $\tilde{\mathbf{q}}\equiv(0,0,q)$. Explicit expressions for $L^{\beta\alpha}_{v_e v_e}$, etc., are given in Appendix B.

The cross section (30), summed over all possible initial and final electron states, is

$$d\sigma^{(\nu)}=\frac{G_{\mathrm{F}}^2}{(2\pi)^2 32m_eE_{\nu_i}}\int\delta(E^{(\nu)}_{fi})E_{\nu_f}dE_{\nu_f}d\Omega_{\nu_f}dE_f$$
$$\times L_{fi}(\tilde{\mathbf{q}},p_{\nu_i},p_{\nu_f}), \quad (66)$$

where

$$L_{fi}(\tilde{\mathbf{q}},p_{\nu_i},p_{\nu_f})=\mathrm{Re}[L^{(e)}_{fi}(\tilde{\mathbf{q}})^{\beta\alpha}]\mathrm{Re}[L^{(\nu)}(p_{\nu_i},p_{\nu_f})_{\beta\alpha}]$$
$$-\mathrm{Im}[L^{(e)}_{fi}(\tilde{\mathbf{q}})^{\beta\alpha}]\mathrm{Im}[L^{(\nu)}(p_{\nu_i},p_{\nu_f})_{\beta\alpha}], \quad (67)$$

and we have used, for final electron states normalized according to (C9), $d\rho_f^{(e)}=dE_f/m_e$. Introducing

$$R^{\beta\alpha}(\tilde{\mathbf{q}})=\int dE_f\delta(E^{(\nu)}_{fi})L^{(e)}_{fi}(\tilde{\mathbf{q}})^{\beta\alpha}$$
$$=\sum_{\kappa_f,\mu_f,\mu_i}\int dE_f\delta(E^{(\nu)}_{fi})N^{\beta}_{fi}(\tilde{\mathbf{q}})^*N^{\alpha}_{fi}(\tilde{\mathbf{q}}), \quad (68)$$

then the cross section has the form used by [16,17] with their response functions (13) corresponding to (68).

Of particular interest is the energy spectrum of the ionization electrons

$$\frac{d\sigma^{(\nu)}}{dE_f}=\frac{G_{\mathrm{F}}^2}{(2\pi)^2}\frac{E_{\nu_f}}{32m_eE_{\nu_i}}\int d\Omega_{\nu_f}L_{fi}(\tilde{\mathbf{q}},p_{\nu_i},p_{\nu_f}) \quad (69)$$

where, in (69), it is understood that $E_{\nu_f}=E_i+E_{\nu_i}-E_f$. As the coordinate system has been chosen such that $\mathbf{p}_{\nu_i}$, $\mathbf{p}_{\nu_f}$ and $\mathbf{q}$ lie in the x–z plane with $\mathbf{q}$ along the Oz axis, the

integration over Ω_{ν_f} becomes $-2\pi\int d(\cos\theta)$ where θ is the angle between $\mathbf{p}_{\nu_i}$ and $\mathbf{p}_{\nu_f}$. Noting that $q^2 = E_{\nu_i}^2 + E_{\nu_f}^2 - 2E_{\nu_i}E_{\nu_f}\cos\theta$, then $-d(\cos\theta) = dq^2/(2E_{\nu_i}E_{\nu_f})$, and our final expression for the energy spectrum is

$$\frac{d\sigma^{(\nu)}}{dE_f} = \frac{G_F^2}{8\pi}\frac{1}{16m_eE_{\nu_i}^2}\int dq^2 L_{fi}(\tilde{\mathbf{q}}, p_{\nu_i}, p_{\nu_f}). \quad (70)$$

III. RADIAL MATRIX ELEMENTS

The radial integrals (45) involve the Dirac radial functions $g_{\kappa,E}(r)$ and $f_{\kappa,E}(r)$ for the initial bound electron and the final continuum electron. For a Coulombic potential $V(r) = -\alpha Z/r$, the radial Dirac equations (38) have analytic solutions [23] in terms of confluent hypergeometric functions ${}_1F_1(a,c,z)$.

In this study we consider the scattering by electrons in the ground states of H, He and Ne. As these systems involve only K- and L- shell electrons, we can use the simplified expressions

$$\begin{pmatrix} g_{\kappa_i,E_i}(r) \\ f_{\kappa_i,E_i}(r) \end{pmatrix} = N_i \begin{pmatrix} \sqrt{m_e + E_i} \\ -\sqrt{m_e - E_i} \end{pmatrix} (2\lambda_i r)^{\gamma_i} e^{-\lambda_i r} \times \left[\begin{pmatrix} c_0 \\ a_0 \end{pmatrix} + \begin{pmatrix} c_1 \\ a_1 \end{pmatrix} \lambda_i r \right] \quad (71)$$

where

$$\lambda_i \equiv \sqrt{m_e^2 - E_i^2}, \qquad \gamma_i \equiv \sqrt{\kappa_i^2 - (\alpha Z)^2} \quad (72)$$

and the initial state energy E_i is

$$E_{n,\kappa_i} = m_e\left[1 + \left(\frac{\alpha Z}{n - |\kappa_i| + \gamma_i}\right)^2\right]^{-1/2}. \quad (73)$$

The dimensionless coefficients $(c_{0,1}, a_{0,1}, N_i)$ for the K-shell $(n=1,\kappa_i=-1)$, L_I-subshell $(n=2,\kappa_i=-1)$, L_{II}-subshell $(n=2,\kappa_i=+1)$ and L_{III}-subshell $(n=2,\kappa_i=-2)$ are tabulated in [23]. (Note that [23] uses relativistic units $\hbar = c = m_e = 1$.) Since $\alpha Z \ll 1$, the initial state binding energy $\epsilon_i \equiv m_e - E_i$ can be approximated as $(\alpha Z)^2 m_e/2$ for K-shell electrons and $(\alpha Z)^2 m_e/8$ for L-shell electrons. The screening effects of the electrons in the filled K- shell (for He and Ne), and L-subshells (for Ne) are represented by an effective nuclear charge $Z_{\rm eff} = Z - s_i$, a procedure that should be reasonable for small principal quantum number n and small $n-l$ [26]. These screening constants s_i, taken from the fits [27] of Dirac single electron eigenfunctions to empirical binding energies, are 0.656 (K-shell), 2.016 (L_I-subshell), 6.254 (L_{II}-subshell) and 7.482 (L_{III}-subshell).

The final electron continuum states, energy normalized according to (C9), are

$$\begin{pmatrix} g_{\kappa_f,E_f}(r) \\ f_{\kappa_f,E_f}(r) \end{pmatrix} = N_f \begin{pmatrix} \sqrt{E_f + m_e} \\ i\sqrt{E_f - m_e} \end{pmatrix} (2p_f r)^{\gamma_f}[(\gamma_f + iy) \times e^{-ip_f r + i\eta}\,{}_1F_1(a,c,2ip_f r) \pm \text{c.c}], \quad (74)$$

where

$$\gamma_f \equiv \sqrt{\kappa_f^2 - (\alpha Z)^2}, \quad p_f \equiv \sqrt{E_f^2 - m_e^2}, \quad y \equiv \frac{\alpha Z E_f}{p_f}, \quad (75)$$

and

$$e^{2i\eta} = -\frac{\kappa_f - iym_e/E_f}{\gamma_f + iy}. \quad (76)$$

The dimensionless normalization constant is

$$N_f = \frac{e^{\pi y/2}}{2}\sqrt{\frac{m_e}{\pi p_f}}\frac{|\Gamma(\gamma_f + iy)|}{\Gamma(2\gamma_f + 1)}. \quad (77)$$

The parameters in the hypergeometric function are $a = \gamma_f + 1 + iy$ and $c = 2\gamma_f + 1$. Since a and $z \equiv 2ip_f r$ are complex, the computation of ${}_1F_1(a,c,z)$ involves the summation of a slowly convergent complex series for each required value of z. Consequently we choose to integrate the Dirac equation directly. For each shell and subshell calculation, the continuum state electrons are assumed to move in the same potential as the bound state electrons [28].

Details of the computation of the continuum radial functions and the radial integrals (45) are given in Appendix C.

IV. EVALUATION OF CROSS SECTIONS

The cross section involves the contraction of the electron tensor $L_{fi}^{(e)}(\mathbf{q})^{\beta\alpha}$, given by (65), with the neutrino tensor $L_{\beta\alpha}^{(\nu)}(p_{\nu_i}, p_{\nu_f})$ given by (32). From (64), we need only the diagonal elements (β,β) and the off-diagonal elements $(\beta,\alpha) = (1,2),(2,1),(0,3),(3,0)$ of the two tensors.

The summation over l in the electron tensor is constrained by the conditions $\bar{\Delta}(l_3,l_4,l)$ where $l_3 = (l_f, l_f')$ and $l_4 = (l_i, l_i')$. Here $\bar{\Delta}(a,b,c)$ implies $|a-b| \le c \le a+b$, together with $a+b+c =$ even integer. Similar constraints apply to the summation over $\bar{l}$. As l_i has the values 0 or 1, and l_i' the values 0, 1 or 2, the number of terms in these summations is quite small. However, the summation over κ_f is unconstrained, with convergence coming from the decreasing overlap between the initial bound and final continuum electron eigenfunctions with increasing κ_f in the radial integrals.

For $\kappa_i = -1$, the special case

$$A_{\bar{l}l}^{(I,I)}(l_f,0,l_f,0) = A_{\bar{l}l}^{(\lambda,\lambda)}(l_f,0,l_f,0) = \delta_{\bar{l},l}\delta_{l,l_f}\frac{2j_f+1}{(2l_f+1)^2} \tag{78}$$

can be used to check the evaluation of the A coefficients. A similar result holds for $\kappa_i = 1$ with l_f replaced by l'_f.

The required elements of the neutrino tensor are calculated from (32) where, with our choice of coordinate system, $\mathbf{p}_{\nu_i} = (E_{\nu_i}\sin(\gamma-\theta), 0, E_{\nu_i}\cos(\gamma-\theta))$ and $\mathbf{p}_{\nu_f} = (E_{\nu_f}\sin\gamma, 0, E_{\nu_f}\cos\gamma)$. Here, γ is the angle between $\mathbf{q}$ and $\mathbf{p}_{\nu_f}$ and is related to the scattering angle θ via

$$\tan\gamma = \frac{\sin\theta}{\cos\theta - E_{\nu_f}/E_{\nu_i}}. \tag{79}$$

These elements can be expressed [16] in terms of the energy transfer $T \equiv E_{\nu_i} - E_{\nu_f}$ and the quantity $Q^2 \equiv q^2 - T^2$, that is, $Q^2 = -t > 0$. Explicitly,

$$\begin{aligned}
L^{(\nu)0,0} &= 16E_{\nu_i}E_{\nu_f}\cos^2\left(\frac{\theta}{2}\right),\\
L^{(\nu)1,1} &= 16E_{\nu_i}E_{\nu_f}\cos^2\left(\frac{\theta}{2}\right)\left[\tan^2\left(\frac{\theta}{2}\right)+\frac{Q^2}{q^2}\right],\\
L^{(\nu)2,2} &= 16E_{\nu_i}E_{\nu_f}\cos^2\left(\frac{\theta}{2}\right)\tan^2\left(\frac{\theta}{2}\right),\\
L^{(\nu)3,3} &= 16E_{\nu_i}E_{\nu_f}\cos^2\left(\frac{\theta}{2}\right)\frac{T^2}{q^2},\\
L^{(\nu)1,2} &= -L^{(\nu)2,1} = -16iE_{\nu_i}E_{\nu_f}\cos^2\left(\frac{\theta}{2}\right)\tan\left(\frac{\theta}{2}\right)\\
&\quad\times\sqrt{\tan^2\left(\frac{\theta}{2}\right)+\frac{Q^2}{q^2}},\\
L^{(\nu)0,3} &= L^{(\nu)3,0} = 16E_{\nu_i}E_{\nu_f}\cos^2\left(\frac{\theta}{2}\right)\frac{T}{q}.
\end{aligned} \tag{80}$$

For antineutrino scattering, $L^{(\bar{\nu})\beta,\alpha} = (L^{(\nu)\beta,\alpha})^*$. The difference between ν_e and $\bar{\nu}_e$ scattering therefore arises solely from the (1,2) and (2,1) components.

V. RESULTS AND DISCUSSION

The energy spectra $d\sigma/dE_f$ of the ionization electrons produced in low energy scattering of electron neutrinos and antineutrinos by atomic electrons have been calculated as a function of the electron kinetic energy $\epsilon_f = E_f - m_e$. Results are obtained for scattering of 5, 10, 20, and 30 keV neutrino energies by the ground state systems H($1s$), He($1s^2$), and Ne($1s^22s^22p^6$) where, for He and Ne, the electrons are considered as independent scattering centers.

The energy spectra are compared to that for scattering from free electrons, for which, in the laboratory frame, $E_i = m_e, \mathbf{p}_{e_i} = 0$ and the kinematic variables simplify to

$$\begin{aligned}
s &= m_e(m_e + 2E_{\nu_i}),\\
u &= m_e(m_e - 2E_{\nu_f}),\\
t &= 2m_e(m_e - E_f).
\end{aligned} \tag{81}$$

Setting $\tilde{m} = m_e$ in (3), the energy spectrum of the scattered electron for ν_e scattering is then [10]

$$\begin{aligned}
\left(\frac{d\sigma^{(\nu)}}{dE_f}\right)_{(\text{Free})} &= \frac{G_F^2 m_e}{8\pi E_{\nu_i}^2}\{(\bar{v}_e-\bar{a}_e)^2E_{\nu_i}^2\\
&\quad+(\bar{v}_e+\bar{a}_e)^2(E_{\nu_i}+m_e-E_f)^2\\
&\quad+m_e(\bar{v}_e^2-\bar{a}_e^2)(m_e-E_f)\},
\end{aligned} \tag{82}$$

where $m_e \le E_f \le m_e + \epsilon_f^{\max}$ and the maximum kinetic energy is

$$\epsilon_f^{\max} = \frac{2E_{\nu_i}^2}{m_e + 2E_{\nu_i}}. \tag{83}$$

For low energy transfers $T \ll E_{\nu_i}$,

$$\begin{aligned}
\left(\frac{d\sigma^{(\nu)}}{dE_f}\right)_{(\text{Free})} &= \frac{G_F^2 m_e}{2\pi}(1+4\sin^2\theta_W+8\sin^4\theta_W)\\
&\quad\times\left[1+O\left(\frac{T}{E_{\nu_i}}\right)\right].
\end{aligned} \tag{84}$$

The total cross section for scattering off free electrons is [10]

$$\begin{aligned}
\sigma_{(\text{Free})}^{(\nu)} &= \frac{G_F^2 m_e E_{\nu_i}}{8\pi}\left[(\bar{v}_e-\bar{a}_e)^2\frac{2E_{\nu_i}}{m_e+2E_{\nu_i}}\right.\\
&\quad+\frac{1}{3}(\bar{v}_e+\bar{a}_e)^2\left\{1-\frac{m_e^3}{(m_e+2E_{\nu_i})^3}\right\}\\
&\quad\left.-(\bar{v}_e^2-\bar{a}_e^2)\frac{2m_eE_{\nu_i}}{(m_e+2E_{\nu_i})^2}\right].
\end{aligned} \tag{85}$$

For $\bar{\nu}_e$ scattering, the interchange $s \leftrightarrow u$ in (3) is equivalent to $\bar{a}_e \leftrightarrow -\bar{a}_e$ in (82) and (85). The low T limit is unaltered.

Energy spectra and total cross sections for ν_e and $\bar{\nu}_e$ scattering by free electrons are given in Table I.

Results for ν_e ($\bar{\nu}_e$) scattering by H are given in Table II (Table III), by He in Table IV (Table V), and by Ne in Table VI (Table VII), respectively. The energy spectra and cross sections are expressed as ratios

TABLE I. Energy spectra $(d\sigma^{(\nu)}/dE_f)_{(\mathrm{Free})}$ of electrons resulting from scattering of incident neutrinos of energy E_{ν_i} by free electrons. The results, in units of 10^{-14} GeV^{-3}, are given as a function of the kinetic energy ϵ_f of the electron. Also shown are the integrated spectra $\sigma^{(\nu)}_{(\mathrm{Free})}$ in units of 10^{-20} GeV^{-2}. Results for scattering of antineutrinos are given in parentheses.

$\epsilon_f/\epsilon_f^{\max}$	$E_{\nu_i} = 5$ (keV)	$E_{\nu_i} = 10$ (keV)	$E_{\nu_i} = 20$ (keV)	$E_{\nu_i} = 30$ (keV)
0.0	2.6029(2.6029)	2.6029(2.6029)	2.6029(2.6029)	2.6029 (2.6029)
0.1	2.4553(2.4471)	2.4571(2.4411)	2.4607(2.4299)	2.4641 (2.4195)
0.2	2.3076(2.2912)	2.3114(2.2794)	2.3185(2.2571)	2.3252 (2.2367)
0.3	2.1599(2.1354)	2.1656(2.1177)	2.1764(2.0846)	2.1865 (2.0543)
0.4	2.0122(1.9796)	2.0198(1.9561)	2.0342(1.9124)	2.0478 (1.8725)
0.5	1.8645(1.8238)	1.8740(1.7946)	1.8921(1.7403)	1.9091 (1.6912)
0.6	1.7168(1.6681)	1.7283(1.6331)	1.7500(1.5686)	1.7705 (1.5104)
0.7	1.5692(1.5123)	1.5825(1.4717)	1.6080(1.3970)	1.6319 (1.3301)
0.8	1.4215(1.3566)	1.4368(1.3104)	1.4660(1.2258)	1.4934 (1.1504)
0.9	1.2738(1.2009)	1.2910(1.1491)	1.3239(1.0547)	1.3550 (0.9712)
1.0	1.1261(1.0452)	1.1453(0.9879)	1.1820(0.8840)	1.2166 (0.7925)
$\epsilon_f^{\max}$ (eV)	95.969	376.65	1451.9	3152.4
$\sigma^{(\nu)}_{(\mathrm{Free})}$	0.31980(0.31590)	1.2483(1.2185)	4.7624(4.5434)	10.241(9.5600)

TABLE II. Energy spectra $d\sigma^{(\nu)}/dE_f$ of the ionization electrons from scattering of incident neutrinos of energy E_{ν_i} by hydrogen. The results are expressed as ratios to the spectra $(d\sigma^{(\nu)}/dE_f)_{(\mathrm{Free})}$ for scattering by free electrons and are given as a function of the kinetic energy ϵ_f of the electron. Results are shown for a Coulombic final electron and, in parentheses, for a free final electron. Also shown are the integrated spectra $\sigma^{(\nu)}$ expressed as a ratio to the integrated spectra $\sigma^{(\nu)}_{(\mathrm{Free})}$ for a free electron.

$\epsilon_f/\epsilon_f^{\max}$	$E_{\nu_i} = 5$ (keV)	$E_{\nu_i} = 10$ (keV)	$E_{\nu_i} = 20$ (keV)	$E_{\nu_i} = 30$ (keV)
0.1	0.7780(0.8467)	0.9472(0.9776)	0.9880(0.9970)	0.9952 (0.9991)
0.2	0.7680(0.9169)	0.9465(0.9877)	0.9877(0.9976)	0.9953 (0.9994)
0.3	0.7482(0.9345)	0.9427(0.9890)	0.9870(0.9976)	0.9952 (0.9995)
0.4	0.7192(0.9354)	0.9368(0.9883)	0.9861(0.9976)	0.9945 (0.9991)
0.5	0.6795(0.9254)	0.9267(0.9857)	0.9849(0.9974)	0.9930 (0.9981)
0.6	0.6273(0.9033)	0.9074(0.9782)	0.9828(0.9968)	0.9906 (0.9961)
0.7	0.5624(0.8664)	0.8669(0.9574)	0.9773(0.9942)	0.9868 (0.9931)
0.8	0.4872(0.8125)	0.7819(0.9022)	0.9545(0.9796)	0.9780 (0.9864)
0.9	0.4075(0.7428)	0.6286(0.7797)	0.8376(0.8877)	0.9183 (0.9383)
1.0	0.3308(0.6630)	0.4256(0.5840)	0.4629(0.5367)	0.4643 (0.5122)
$\epsilon_f^{\max}$ (eV)	95.969	376.65	1451.9	3152.4
$\sigma^{(\nu)}/\sigma^{(\nu)}_{(\mathrm{Free})}$	0.6626(0.8696)	0.8811(0.9472)	0.9568(0.9741)	0.9729(0.9802)

$$R^{(\nu)}(E_f) = \frac{d\sigma^{(\nu)}/dE_f}{Z(d\sigma^{(\nu)}/dE_f)_{(\mathrm{Free})}}, \tag{86}$$

and $\sigma^{(\nu)}/Z\sigma^{(\nu)}_{(\mathrm{Free})}$, to the corresponding quantities for scattering by Z free electrons. Also listed are results for the case where the final continuum electron is treated as free, for which the radial eigenfunctions normalized according to (C9) are

$$\begin{pmatrix} g_{\kappa_f,E_f}(r) \\ f_{\kappa_f,E_f}(r) \end{pmatrix} = \sqrt{\frac{p_f m_e}{\pi}} \begin{pmatrix} \sqrt{E_f + m_e}\, r j_{l_f}(p_f r) \\ S_{\kappa_f}\sqrt{E_f - m_e}\, r j_{l'_f}(p_f r) \end{pmatrix}, \tag{87}$$

where $S_{\kappa_f} \equiv \kappa_f/|\kappa_f|$.

The energy spectra of electrons resulting from the scattering of neutrinos by free electrons are shown in Fig. 1, and the energy spectra ratios for scattering of neutrinos by H, He, and Ne are shown in Figs 2–4 respectively. Plots for scattering of antineutrinos differ only very slightly from those for scattering by neutrinos

TABLE III. Energy spectra $d\sigma^{(\bar{\nu})}/dE_f$ of the ionization electrons from scattering of incident antineutrinos of energy E_{ν_i} by hydrogen. The results are expressed as ratios to the spectrum $(d\sigma^{(\bar{\nu})}/dE_f)_{(\mathrm{Free})}$ for scattering by free electrons and are given as a function of the kinetic energy ϵ_f of the electron. Results are shown for a Coulombic final electron and, in parentheses, for a free final electron. Also shown are the integrated spectra $\sigma^{(\bar{\nu})}$ expressed as a ratio to the integrated spectra $\sigma^{(\bar{\nu})}_{(\mathrm{Free})}$ for a free electron.

$\epsilon_f/\epsilon_f^{\max}$	$E_{\nu_i} = 5$ (keV)	$E_{\nu_i} = 10$ (keV)	$E_{\nu_i} = 20$ (keV)	$E_{\nu_i} = 30$ (keV)
0.1	0.7690(0.8448)	0.9415(0.9768)	0.9855(0.9969)	0.9938 (0.9993)
0.2	0.7587(0.9148)	0.9401(0.9868)	0.9850(0.9977)	0.9940 (0.9999)
0.3	0.7389(0.9324)	0.9356(0.9879)	0.9840(0.9979)	0.9938 (1.000)
0.4	0.7105(0.9336)	0.9287(0.9870)	0.9827(0.9978)	0.9930 (1.000)
0.5	0.6720(0.9244)	0.9178(0.9841)	0.9807(0.9975)	0.9912 (0.9992)
0.6	0.6219(0.9043)	0.8985(0.9768)	0.9775(0.9965)	0.9882 (0.9972)
0.7	0.5599(0.8706)	0.8599(0.9576)	0.9578(0.9934)	0.9833 (0.9937)
0.8	0.4882(0.8213)	0.7804(0.9074)	0.9485(0.9795)	0.9731 (0.9862)
0.9	0.4123(0.7577)	0.6361(0.7943)	0.8416(0.8966)	0.9179 (0.9422)
1.0	0.3393(0.6852)	0.4415(0.6093)	0.4844(0.5693)	0.4880 (0.5399)
$\epsilon_f^{\max}$ (eV)	95.969	376.65	1451.9	3152.4
$\sigma^{(\bar{\nu})}/\sigma^{(\bar{\nu})}_{(\mathrm{Free})}$	0.6590(0.8717)	0.8794(0.9505)	0.9576(0.9779)	0.9749(0.9843)

TABLE IV. Energy spectra $d\sigma^{(\nu)}/dE_f$ of the ionization electrons from scattering of incident neutrinos of energy E_{ν_i} by helium. The results are expressed as ratios to the spectra $2(d\sigma^{(\nu)}/dE_f)_{(\mathrm{Free})}$ for scattering by two free electrons and are given as a function of the kinetic energy ϵ_f of the electron. Results are shown for a Coulombic final electron and, in parentheses, for a free final electron. Also shown are the integrated spectra $\sigma^{(\nu)}$ expressed as a ratio to the integrated spectra $2\sigma^{(\nu)}_{(\mathrm{Free})}$ for two free electrons.

$\epsilon_f/\epsilon_f^{\max}$	$E_{\nu_i} = 5$ (keV)	$E_{\nu_i} = 10$ (keV)	$E_{\nu_i} = 20$ (keV)	$E_{\nu_i} = 30$ (keV)
0.1	0.6179(0.7209)	0.9020(0.9444)	0.9778(0.9929)	0.9910 (0.9977)
0.2	0.5983(0.8258)	0.9000(0.9719)	0.9774(0.9951)	0.9910 (0.9983)
0.3	0.5705(0.8607)	0.8920(0.9766)	0.9761(0.9954)	0.9907 (0.9986)
0.4	0.5358(0.8692)	0.8787(0.9757)	0.9743(0.9952)	0.9902 (0.9987)
0.5	0.4952(0.8626)	0.8568(0.9697)	0.9715(0.9947)	0.9894 (0.9986)
0.6	0.4498(0.8444)	0.8200(0.9549)	0.9659(0.9929)	0.9879 (0.9982)
0.7	0.4015(0.8164)	0.7585(0.9222)	0.9512(0.9857)	0.9842 (0.9964)
0.8	0.3528(0.7801)	0.6627(0.8579)	0.9031(0.9549)	0.9680 (0.9861)
0.9	0.3062(0.7385)	0.5331(0.7511)	0.7513(0.8359)	0.8671 (0.9068)
1.0	0.2641(0.6953)	0.3904(0.6088)	0.4472(0.5492)	0.4607 (0.5268)
$\epsilon_f^{\max}$ (eV)	95.969	376.65	1451.9	3152.4
$\sigma^{(\nu)}/\sigma^{(\nu)}_{(\mathrm{Free})}$	0.5019(0.7988)	0.8129(0.9235)	0.9343(0.9644)	0.9635(0.9769)

and are not shown. The energy spectra ratios for scattering of 10, 20, and 30 keV neutrinos by H, He, and Ne become constant at low kinetic energies and can safely be extrapolated to lower kinetic energies by assuming the ratios are constant.

The calculations involve a sum over κ_f with convergence decreasing with increasing ϵ_f. The choice $|\kappa_f| \leq 20$ for $E_{\nu_i} = 5$ keV, $|\kappa_f| \leq 30$ for $E_{\nu_i} = 10$ keV, and $|\kappa_f| \leq 50$ for $E_{\nu_i} = 20$ keV, gave convergence of much better than 1×10^{-4} for each energy spectrum. For the larger electron kinetic energies at $E_{\nu_i} = 30$ keV, the imposed practical limit $|\kappa_f| \leq 50$ gave convergence of better than 1×10^{-4} for $\epsilon_f \lesssim 1.5$ keV in the spectrum but, for higher energies, the convergence decreased to 1×10^{-3} at $\epsilon_f^{\max}$, so the numbers shown for the high energy end of the spectra are slight underestimates. For Ne, this decrease in convergence to below 1×10^{-4} only occurred for the L_{III} subshell.

It is evident in the calculated spectra that binding effects increase strongly with atomic number, are greatest for low E_{ν_i} and, for each E_{ν_i}, most significant at the high electron energy end of the spectrum. As expected, the binding effects are less for a free final electron than for a Coulombic final electron. For Ne, the binding effects were strongest for the K shell. The K shell results also showed the greatest

TABLE V. Energy spectra $d\sigma^{(\bar{\nu})}/dE_f$ of the ionization electrons from scattering of incident antineutrinos of energy E_{ν_i} by helium. The results are expressed as ratios to the spectrum $2(d\sigma^{(\bar{\nu})}/dE_f)_{(\mathrm{Free})}$ for scattering by two free electrons and are given as a function of the kinetic energy ϵ_f of the electron. Results are shown for a Coulombic final electron and, in parentheses, for a free final electron. Also shown are the integrated spectra $\sigma^{(\bar{\nu})}$ expressed as a ratio to the integrated spectra $2\sigma^{(\bar{\nu})}_{(\mathrm{Free})}$ for two free electrons.

$\epsilon_f/\epsilon_f^{\max}$	$E_{\nu_i} = 5$ (keV)	$E_{\nu_i} = 10$ (keV)	$E_{\nu_i} = 20$ (keV)	$E_{\nu_i} = 30$ (keV)
0.1	0.6070(0.7180)	0.8919(0.9427)	0.9729(0.9925)	0.9880 (0.9977)
0.2	0.5877(0.8226)	0.8889(0.9699)	0.9720(0.9949)	0.9879 (0.9987)
0.3	0.5608(0.8579)	0.8800(0.9744)	0.9700(0.9951)	0.9874 (0.9991)
0.4	0.5274(0.8673)	0.8659(0.9732)	0.9672(0.9947)	0.9864 (0.9994)
0.5	0.4885(0.8624)	0.8441(0.9674)	0.9630(0.9938)	0.9848 (0.9992)
0.6	0.4454(0.8469)	0.8090(0.9539)	0.9560(0.9914)	0.9821 (0.9984)
0.7	0.3997(0.8227)	0.7517(0.9249)	0.9408(0.9842)	0.9766 (0.9959)
0.8	0.3538(0.7917)	0.6629(0.8678)	0.8967(0.9571)	0.9600 (0.9856)
0.9	0.3102(0.7569)	0.5423(0.7717)	0.7597(0.8520)	0.8705 (0.9167)
1.0	0.2712(0.7224)	0.4074(0.6413)	0.4732(0.5848)	0.4906 (0.5637)
$\epsilon_f^{\max}$ (eV)	95.969	376.65	1451.9	3152.4
$\sigma^{(\bar{\nu})}/\sigma^{(\bar{\nu})}_{(\mathrm{Free})}$	0.4975(0.8008)	0.8091(0.9272)	0.9340(0.9696)	0.9649(0.9818)

TABLE VI. Energy spectra $d\sigma^{(\nu)}/dE_f$ of the ionization electrons from scattering of incident neutrinos of energy E_{ν_i} by neon. The results are expressed as ratios to the spectra $10(d\sigma^{(\nu)}/dE_f)_{(\mathrm{Free})}$ for scattering by 10 free electrons and are given as a function of the kinetic energy ϵ_f of the electron. Results are shown for a Coulombic final electron and, in parentheses, for a free final electron. Also shown are the integrated spectra $\sigma^{(\nu)}$ expressed as a ratio to the integrated spectra $10\sigma^{(\nu)}_{(\mathrm{Free})}$ for 10 free electrons.

$\epsilon_f/\epsilon_f^{\max}$	$E_{\nu_i} = 5$ (keV)	$E_{\nu_i} = 10$ (keV)	$E_{\nu_i} = 20$ (keV)	$E_{\nu_i} = 30$ (keV)
0.1	0.09921(0.2905)	0.2847(0.4001)	0.4694(0.5130)	0.5697 (0.5901)
0.2	0.09333(0.2971)	0.2783(0.4188)	0.4789(0.5533)	0.5793 (0.6365)
0.3	0.08777(0.2892)	0.2685(0.4277)	0.4818(0.5755)	0.5798 (0.6561)
0.4	0.08329(0.2760)	0.2554(0.4310)	0.4798(0.5882)	0.5757 (0.6641)
0.5	0.08068(0.2594)	0.2384(0.4283)	0.4720(0.5951)	0.5691 (0.6652)
0.6	0.08027(0.2411)	0.2164(0.4167)	0.4548(0.5967)	0.5597 (0.6617)
0.7	0.08149(0.2244)	0.1908(0.3922)	0.4225(0.5885)	0.5424 (0.6536)
0.8	0.08286(0.2131)	0.1696(0.3555)	0.3641(0.5543)	0.4997 (0.6314)
0.9	0.08277(0.2100)	0.1623(0.3235)	0.2773(0.4672)	0.3880 (0.5438)
1.0	0.08036(0.2161)	0.1578(0.3157)	0.2334(0.3973)	0.2720 (0.4043)
$\epsilon_f^{\max}$ (eV)	95.969	376.65	1451.9	3152.4
$\sigma^{(\nu)}/\sigma^{(\nu)}_{(\mathrm{Free})}$	0.08732(0.2613)	0.2383(0.3998)	0.4375(0.5494)	0.5395(0.6220)

enhancement from the use of Coulombic final electron states. To a lesser extent, this was also the case for the L_I subshell at the lower neutrino energies.

The sharp decrease in the spectra at the high energy end is a consequence of the very small range of the q^2 integration in (70) for this region. Since $q_{\max} = E_{\nu_i} + E_{\nu_f}$ and $q_{\min} = E_{\nu_i} - E_{\nu_f}$, the range $2E_{\nu_f}$ is minimized at $E_f^{\max}$. Also, for this region, $q \approx E_{\nu_i}$, so that the high energy tail will increase as E_{ν_i} increases.

The shape of the Coulombic and free final electron energy spectra ratios $R(E_f)$ differ slightly. The Coulombic final electron spectra ratios are approximately constant over the region just above $\epsilon_f^{\min} = 0.1\epsilon_f^{\max}$ before decreasing, in most cases, monotonically, whereas the free final electron spectra ratios increase initially with ϵ_f to a small peak before decreasing monotonically.

Existing calculations [10,11] model the scattering by a bound electron as scattering from a free electron with effective mass $\tilde{m}$. The cross section obtained from (5) is

$$d\sigma^{(\mathrm{Atom})} = \frac{1}{4E_{\nu_i}E_i}\int \frac{d^3\mathbf{p}_{e_i}}{(2\pi)^3}|\Psi_{n_i l_i m_i}(\mathbf{p}_{e_i})|^2 \times |F(\nu_e e^- \to \nu_e e^-)|^2 d\Phi^{(2)}(p_{e_f}, p_{\nu_f}), \quad (88)$$

where the two-body phase space is

TABLE VII. Energy spectra $d\sigma^{(\bar{\nu})}/dE_f$ of the ionization electrons from scattering of incident antineutrinos of energy E_{ν_i} by neon. The results are expressed as ratios to the spectrum $10(d\sigma^{(\bar{\nu})}/dE_f)_{(\mathrm{Free})}$ for scattering by 10 free electrons and are given as a function of the kinetic energy ϵ_f of the electron. Results are shown for a Coulombic final electron and, in parentheses, for a free final electron. Also shown are the integrated spectra $\sigma^{(\bar{\nu})}$ expressed as a ratio to the integrated spectra $10\sigma^{(\bar{\nu})}_{(\mathrm{Free})}$ for 10 free electrons.

$\epsilon_f/\epsilon_f^{\max}$	$E_{\nu_i} = 5$ (keV)	$E_{\nu_i} = 10$ (keV)	$E_{\nu_i} = 20$ (keV)	$E_{\nu_i} = 30$ (keV)
0.1	0.09751(0.2881)	0.2780(0.3981)	0.4588(0.5100)	0.5539 (0.5865)
0.2	0.09183(0.2946)	0.2721(0.4169)	0.4686(0.5509)	0.5651 (0.6338)
0.3	0.08653(0.2870)	0.2630(0.4260)	0.4716(0.5747)	0.5675 (0.6553)
0.4	0.08230(0.2746)	0.2507(0.4299)	0.4700(0.5894)	0.5656 (0.6661)
0.5	0.07993(0.2592)	0.2349(0.4284)	0.4630(0.5987)	0.5611 (0.6711)
0.6	0.07975(0.2424)	0.2145(0.4191)	0.4479(0.6036)	0.5538 (0.6724)
0.7	0.08126(0.2274)	0.1909(0.3982)	0.4194(0.6005)	0.5397 (0.6705)
0.8	0.08310(0.2179)	0.1718(0.3667)	0.3669(0.5751)	0.5036 (0.6577)
0.9	0.08373(0.2171)	0.1664(0.3405)	0.2876(0.5015)	0.4033 (0.5863)
1.0	0.08234(0.2263)	0.1650(0.3406)	0.2509(0.4474)	0.3138 (0.4671)
$\epsilon_f^{\max}$ (eV)	95.969	376.65	1451.9	3152.4
$\sigma^{(\bar{\nu})}/\sigma^{(\bar{\nu})}_{(\mathrm{Free})}$	0.08669(0.2586)	0.2366(0.4029)	0.4351(0.5558)	0.5375(0.6309)

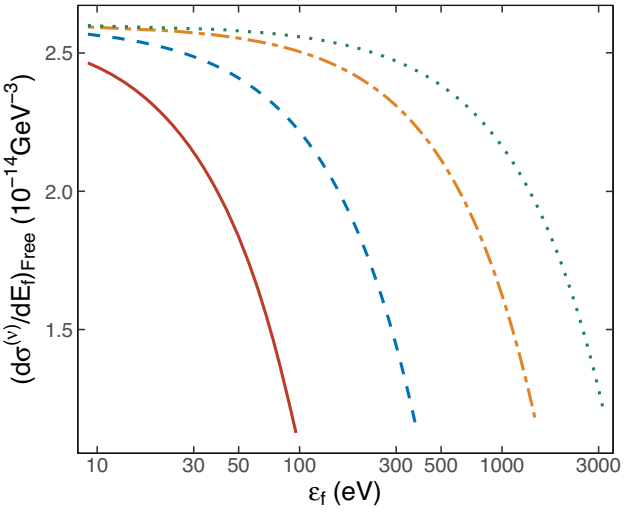

FIG. 1. Energy spectra $(d\sigma^{(\nu)}/dE_f)_{(\mathrm{Free})}$ [Eq. (82)], as a function of electron kinetic energy ϵ_f, of electrons resulting from scattering of neutrinos by free electrons. Results are shown for scattering of 5 keV (solid line), 10 keV (dashed line), 20 keV (dash-dotted line), and 30 keV (dotted line) incident neutrino energies.

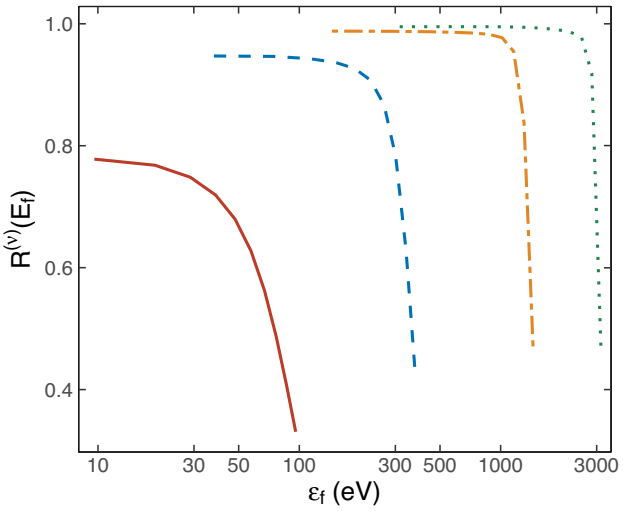

FIG. 2. Energy spectra ratios $R^{(\nu)}(E_f)$ [Eq. (86)], as a function of electron kinetic energy ϵ_f, of ionization electrons resulting from scattering of neutrinos by ground state hydrogen. Results are shown for scattering of 5 keV (solid line), 10 keV (dashed line), 20 keV (dash-dotted line), and 30 keV (dotted line) incident neutrino energies.

$$d\Phi^{(2)}(p_{e_f}, p_{\nu_f}) = \frac{1}{8\pi}\frac{1}{s-\tilde{m}^2}\,dt. \tag{89}$$

The ejected electron energy spectrum is then

$$\frac{d\sigma^{(\mathrm{Atom})}}{dE_f} = \frac{1}{32\pi E_{\nu_i} E_i}\int \frac{d^3\mathbf{p}_{e_i}}{(2\pi)^3}|\Psi_{n_i l_i m_i}(\mathbf{p}_{e_i})|^2 \times |F(\nu_e e^- \to \nu_e e^-)|^2 \frac{1}{s-\tilde{m}^2}\frac{dt}{dE_f}. \tag{90}$$

In the rest frame of the atom, with the incoming neutrino along Oz and the outgoing electron lying in the Oxz plane,

$$s = \tilde{m}^2 + 2E_{\nu_i}(E_i - p_{e_i}\cos\theta_{e_i}) \tag{91}$$

and

$$t = 2E_{\nu_i}(E_f - p_{e_f}\cos\theta_{e_f} - E_i - p_{e_i}\cos\theta_{e_i}). \tag{92}$$

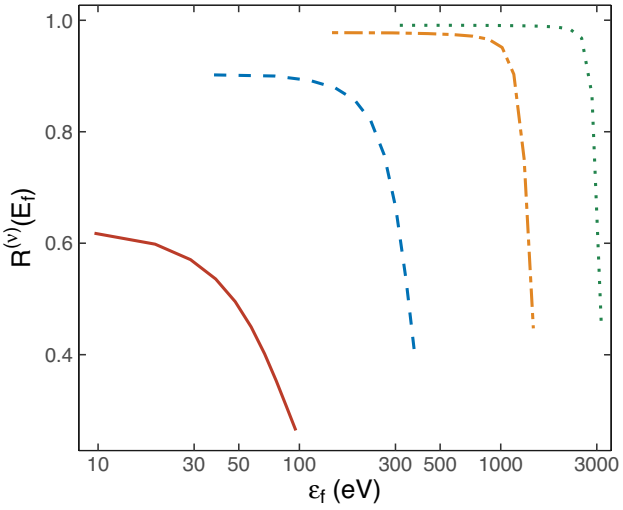

FIG. 3. Energy spectra ratios $R^{(\nu)}(E_f)$ [Eq. (86)], as a function of electron kinetic energy ϵ_f, of ionization electrons resulting from scattering of neutrinos by ground state helium. Results are shown for scattering of 5 keV (solid line), 10 keV (dashed line), 20 keV (dash-dotted line), and 30 keV (dotted line) incident neutrino energies.

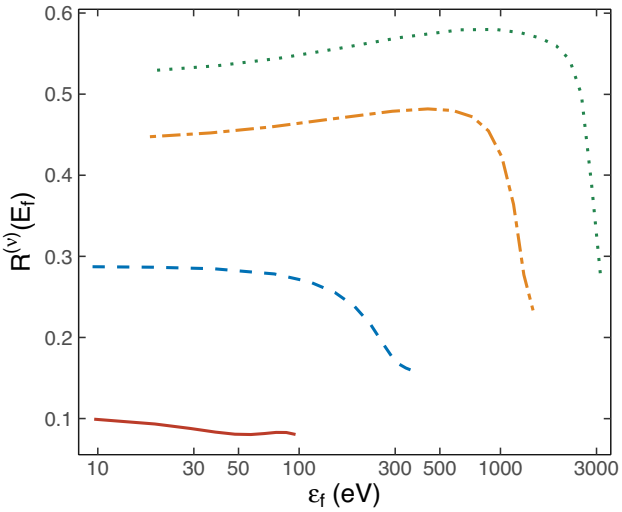

FIG. 4. Energy spectra ratios $R^{(\nu)}(E_f)$ [Eq. (86)], as a function of electron kinetic energy ϵ_f, of ionization electrons resulting from scattering of neutrinos by ground state neon. Results are shown for scattering of 5 keV (solid line), 10 keV (dashed line), 20 keV (dash-dotted line), and 30 keV (dotted line) incident neutrino energies.

The collision kinematics restrict the range of E_f to $E_f^{(2)} \leq E_f \leq E_f^{(1)}$ where [11] the limits $E_f^{(1,2)}$ depend on $\mathbf{p}_{e_i}$.

The energy spectra ratios calculated by [11] have a similar shape to the free final electron spectra ratios calculated here in that the ratios increase initially to a small peak before decreasing monotonically. The present free final electron ratios, however, differ significantly in magnitude to those of [11] and have a much smoother energy dependence.

The integrated cross sections

$$\sigma^{(\nu)} = \int_{E_l}^{E_u} dE_f \frac{d\sigma^{(\nu)}}{dE_f}, \tag{93}$$

where $E_l = m_e$ and $E_u = m_e + \epsilon_f^{\max}$, can be estimated from the calculated energy spectra. As these spectra were only calculated for $E_f \geq m_e + 0.1\epsilon_f^{\max}$, we assume the spectra at $E_f = m_e$ are the same as at $m_e + 0.1\epsilon_f^{\max}$. This assumes the lower energy part of the spectrum is flat. These integrated cross sections are given in the tables, expressed as ratios to the integrated cross sections $Z\sigma^{(\nu)}_{(\mathrm{Free})}$ [Eq. (85)] for Z free electrons.

VI. SUMMARY AND CONCLUSIONS

The energy spectra $d\sigma/dE_f$ of the ionization electrons produced in the scattering of electron neutrinos and antineutrinos with energies 5, 10, 20 and 30 keV by atomic electrons have been calculated for scattering by the ground state systems H$(1s)$, He$(1s^2)$, and Ne$(1s^2 2s^2 2p^6)$ where, for He and Ne, the electrons are considered as independent scattering centers. Results are also obtained for the integrated cross sections.

The present calculations maintain the full collision dynamics by formulating the scattering in configuration space using the bound interaction picture, rather than the usual formulation in the interaction picture in momentum space as appropriate to scattering by free electrons. The energy spectra are expressed as an integral over the momentum transfer q from the neutrino or antineutrino to the atomic system. The integrand is the contraction of the second rank neutrino tensor $L^{(\nu)}$ [Eq. (32)] or antineutrino tensor $L^{(\tilde{\nu})}$ [Eq. (33)], and the second rank electron tensor $L^{(e)}$ [Eq. (65)]. This electron tensor involves radial integrals over Dirac central field radial eigenfunctions for the initial bound electron and final continuum electron, together with a spherical Bessel function arising from the momentum transfer. Screened point-Coulomb radial eigenfunctions have been used, with the continuum state eigenfunctions calculated by direct integration of the Dirac equations.

The calculated energy spectra have been expressed as ratios to the energy spectra for scattering by free electrons. Binding effects increase strongly with atomic number, are largest for low E_{ν_i} and, for each E_{ν_i}, greatest at the high electron energy end of the spectrum. The most extreme effects of binding are for $E_{\nu_i} = 5$ keV scattering by Ne where the ratios are less than 0.1. The energy spectra have been calculated for both a Coulombic final electron state and a free final electron state. The results indicate that the binding effects from the continuum state of the final electron are significant and can be comparable to those arising from

the bound initial electron state. This especially occurs at the high energy end of the spectra for scattering of 5 and 10 keV neutrinos and antineutrinos. As the continuum radial eigenfunctions increase as r^{γ_f} until the point $r_s \approx |\kappa_f|/p_f$ where they become oscillatory (see Appendix C), the continuum state for high E_f and p_f contributes strongly at small distances where the Coulomb interaction is significant. All existing calculations assume a free final electron and therefore under estimate the total binding effects.

The neutrino and antineutrino energy spectra are very similar, with the small difference of $\lesssim 1\%$ arising from the (1,2) and (2,1) elements of the lepton tensor $L^{(\nu)\beta,\alpha}$. In all cases the free electron and bound electron energy spectra for neutrino scattering are higher than those for antineutrinos, although the ratios at the high energy end of the spectra do not reflect this.

The results for the Ne energy spectra show that binding effects are still very significant at $E_{\nu_i} = 30$ keV, the integrated spectra ratios being $\lesssim 0.6$. This suggests the calculations should be extended to higher neutrino energies for this element. However, this would require a substantial increase in the maximum value of $|\kappa_f|$ used as the κ_f convergence is very slow at higher energies, which is not practical. As the results form a monotonic sequence for increasing values of κ_f, a convergence acceleration technique such as the θ-algorithm [29] may be beneficial.

The formalism and techniques developed in the present calculations have assumed the atomic electrons for $Z \neq 1$ are in a closed shell or subshell [see Eq. (54)]. They can be readily applied to other closed shell or subshell atomic systems provided these systems can be represented by central field eigenfunctions. Only the calculation of the radial integrals would require modification to deal with non-Coulombic self-consistent relativistic radial eigenfunctions.

APPENDIX A: SCATTERING MATRIX

The second order S operator for the interaction (16) between an electron-neutrino and an electron is

$$S^{(2)} = -\frac{1}{2}\int d^4x_1 \int d^4x_2 T\{\mathcal{L}_I^{\nu_e e}(x_1)\mathcal{L}_I^{\nu_e e}(x_2)\}, \quad \text{(A1)}$$

where T is the time ordering operator. Of relevance to $\nu_e - e$ scattering are the terms

$$S^{(2)}_{\nu_e e} = -\frac{1}{2}\int d^4x_1 \int d^4x_2 T\{\mathcal{L}_I^{\nu_e We}(x_1)\mathcal{L}_I^{\nu_e We}(x_2) + \mathcal{L}_I^{\nu_e Z\nu_e}(x_1)\mathcal{L}_I^{eZe}(x_2) + \mathcal{L}_I^{eZe}(x_1)\mathcal{L}_I^{\nu_e Z\nu_e}(x_2)\}. \quad \text{(A2)}$$

Using Wick's theorem, the three time-ordered terms become

$$T\{\mathcal{L}_I^{\nu_e We}(x_1)\mathcal{L}_I^{\nu_e We}(x_2)\} = \left(\frac{-g}{2\sqrt{2}}\right)^2 \{N[\overline{\nu_e}(x_1)\gamma^\alpha(1-\gamma_5)e(x_1)W_\alpha^{(+)}\underbrace{(x_1)W_\beta^{(-)}}(x_2)\overline{e}(x_2)\gamma^\beta(1-\gamma_5)\nu_e(x_2)] + (x_1 \leftrightarrow x_2)\} \quad \text{(A3)}$$

$$T\{\mathcal{L}_I^{\nu_e Z\nu_e}(x_1)\mathcal{L}_I^{eZe}(x_2)\} = \left(\frac{-g}{4\cos\theta_W}\right)^2 N[\overline{\nu_e}(x_1)\gamma^\alpha(1-\gamma_5)\nu_e(x_1)Z_\alpha\underbrace{(x_1)Z_\beta}(x_2)\overline{e}(x_2)\gamma^\beta(v_e + a_e\gamma_5)e(x_2)] \quad \text{(A4)}$$

$$T\{\mathcal{L}_I^{eZe}(x_2)\mathcal{L}_I^{\nu_e Z\nu_e}(x_1)\} = T\{\mathcal{L}_I^{\nu_e Z\nu_e}(x_1)\mathcal{L}_I^{eZe}(x_2)\}(x_1 \leftrightarrow x_2). \quad \text{(A5)}$$

Here the contracted operators $W_\alpha^{(+)}\underbrace{(x_1)W_\beta^{(-)}}(x_2)$ and $Z_\alpha\underbrace{(x_1)Z_\beta}(x_2)$ are the W and Z gauge boson propagators respectively, which we denote by $iD^A_{\alpha\beta}(x_1, x_2)$ with $A = W$, Z. As x_1 and x_2 are dummy integration variables, the interchanges in (A3) and (A5) produce terms identical to the original terms.

In order to identify the terms in (A3) and (A4) specific to the scattering of electron neutrinos by electrons, the neutrino and electron field operators are expanded in terms of appropriate basis sets of states, with the coefficients identified as the corresponding particle and antiparticle creation and annihilation operators. For the neutrino field we have the usual expansion in terms of neutrino $u^{(s)}(\mathbf{p})$ and antineutrino $v^{(s)}(\mathbf{p})$ plane wave spinors:

$$\nu_e(x) = \nu_e^{(+)}(x) + \nu_e^{(-)}(x), \quad \text{(A6)}$$

where

$$\nu_e^{(+)}(x) = \frac{1}{(2\pi)^3}\sum_{s=\pm 1/2}\int d^3p \frac{1}{2E_\nu} u^{(s)}(\mathbf{p})b_s(\mathbf{p})e^{-ip\cdot x} \quad \text{(A7)}$$

and

$$\nu_e^{(-)}(x) = \frac{1}{(2\pi)^3}\sum_{s=\pm 1/2}\int d^3p \frac{1}{2E_\nu} v^{(s)}(\mathbf{p})d_s^\dagger(\mathbf{p})e^{ip\cdot x}. \quad \text{(A8)}$$

The expansions for the conjugate field $\overline{\nu_e} \equiv \nu_e^\dagger\gamma^0$ are

$$\overline{\nu_e}(x) = \overline{\nu_e}^{(+)}(x) + \overline{\nu_e}^{(-)}(x), \tag{A9}$$

where

$$\overline{\nu_e}^{(+)}(x) = \frac{1}{(2\pi)^3} \sum_{s=\pm 1/2} \int d^3p \frac{1}{2E_\nu} \overline{v}^{(s)}(\mathbf{p}) d_s(\mathbf{p}) e^{-ip\cdot x}. \tag{A10}$$

and

$$\overline{\nu_e}^{(-)}(x) = \frac{1}{(2\pi)^3} \sum_{s=\pm 1/2} \int d^3p \frac{1}{2E_\nu} \overline{u}^{(s)}(\mathbf{p}) b_s^\dagger(\mathbf{p}) e^{ip\cdot x}. \tag{A11}$$

In the above, $b_s(\mathbf{p})$ ($d_s(\mathbf{p})$) are the neutrino (antineutrino) one-particle annihilation operators, and $b_s^\dagger(\mathbf{p})$ ($d_s^\dagger(\mathbf{p})$) the neutrino (antineutrino) one-particle creation operators, for particles with momentum $\mathbf{p}$ and helicity s. Choosing the normalization

$$\begin{aligned} \bar{u}^{(s')}(\mathbf{p}) \gamma^0 u^{(s)}(\mathbf{p}) &= 2p^0 \delta_{s',s}, \\ \bar{v}^{(s')}(\mathbf{p}) \gamma^0 v^{(s)}(\mathbf{p}) &= 2p^0 \delta_{s',s}, \end{aligned} \tag{A12}$$

then the annihilation and creation operators satisfy

$$\begin{aligned} \{b_s(\mathbf{p}), b_{s'}^\dagger(\mathbf{p}'\} &= (2\pi)^3 2p^0 \delta_{s',s} \delta(\mathbf{p} - \mathbf{p}'), \\ \{d_s(\mathbf{p}), d_{s'}^\dagger(\mathbf{p}'\} &= (2\pi)^3 2p^0 \delta_{s',s} \delta(\mathbf{p} - \mathbf{p}'). \end{aligned} \tag{A13}$$

For the electron field, however, the decomposition is in terms of solutions $\phi(x)$ of (15) for an electron in the external field $A^{(\mathrm{ext})}$. Assuming the positive and negative energy solutions $\phi_n^{(\pm)}(x)$ form two distinct sets, each separated from the zero energy by a finite interval, we can make the expansion ($E_n > 0$)

$$e(x) = e^{(+)}(x) + e^{(-)}(x), \tag{A14}$$

where

$$e^{(+)}(x) = \sum_n a_n \phi_n^{(+)}(\mathbf{x}) e^{-iE_n x^0}, \tag{A15}$$

and

$$e^{(-)}(x) = \sum_n c_n \phi_n^{(-)}(\mathbf{x}) e^{iE_n x^0}. \tag{A16}$$

Similarly, for the conjugate field,

$$\bar{e}(x) = \bar{e}^{(+)}(x) + \bar{e}^{(-)}(x), \tag{A17}$$

where

$$\bar{e}^{(+)}(x) = \sum_n c_n^\dagger \bar{\phi}_n^{(+)}(\mathbf{x}) e^{-iE_n x^0}, \tag{A18}$$

and

$$\bar{e}^{(-)}(x) = \sum_n a_n^\dagger \bar{\phi}_n^{(-)}(\mathbf{x}) e^{iE_n x^0}. \tag{A19}$$

Here, n represents the set of quantum numbers, including E_n, specifying the states in the external field, a_n (c_n) are annihilation operators for electrons with positive (negative) energies, and $a_n^\dagger$ ($c_n^\dagger$) are the corresponding creation operators. If the external-field solutions are normalized according to

$$\langle \phi_{n'}^{(\pm)} | \phi_n^{(\pm)} \rangle = \delta_{n',n}, \tag{A20}$$

then these operators satisfy

$$\{a_n, a_{n'}^\dagger\} = \{c_n, c_{n'}^\dagger\} = \delta_{n',n}. \tag{A21}$$

The relevant terms in (A3) are

$$\begin{aligned} T^W(x_1, x_2) = N[&\overline{\nu_e}^{(\mp)}(x_1) V^\alpha e^{(+)}(x_1) i D_{\alpha\beta}^W(x_1, x_2) \\ &\times \bar{e}^{(-)}(x_2) V^\beta \nu_e^{(\pm)}(x_2)], \end{aligned} \tag{A22}$$

where we have defined the vertex factor

$$V^\alpha \equiv \frac{-g}{2\sqrt{2}} \gamma^\alpha (1 - \gamma_5). \tag{A23}$$

From (A4), the terms are

$$\begin{aligned} T^Z(x_1, x_2) = N[&\overline{\nu_e}^{(\mp)}(x_1) V_\nu^\alpha \nu_e^{(\pm)}(x_1) i D_{\alpha\beta}^Z(x_1, x_2) \\ &\times \bar{e}^{(-)}(x_2) V_e^\beta e^{(+)}(x_2)], \end{aligned} \tag{A24}$$

where the vertex factors are

$$V_\nu^\alpha \equiv \frac{-g}{4\cos\theta_W} \gamma^\alpha (1 - \gamma_5), \tag{A25}$$

$$V_e^\beta \equiv \frac{-g}{4\cos\theta_W} \gamma^\beta (v_e + a_e \gamma_5). \tag{A26}$$

The upper (lower) signs on the neutrino field operators in (A22) and (A24) refer to ν_e ($\overline{\nu_e}$) scattering.

Introducing the Fourier transform of the gauge boson propagator

$$D_{\alpha\beta}^A(x_1, x_2) = \frac{1}{(2\pi)^4} \int d^4k D_{\alpha\beta}^A(k) e^{ik\cdot(x_1 - x_2)}, \tag{A27}$$

where

$$iD^A_{\alpha\beta}(k) = -\frac{i}{k^2 - M_A^2 - i\epsilon}\left[g_{\alpha\beta} - \frac{(1-\xi)k_\alpha k_\beta}{k^2 - \xi M_A^2}\right], \tag{A28}$$

and substituting the expansions (A7), (A11), (A15) and (A19) for the field operators in (A18) allows the integrations over dx_1^0, dx_2^0 and dk^0 to be performed, yielding the energy conservation condition $\delta(E'_n + E_\nu - E_n - E'_\nu)$ and the S-operator for W mediated ν_e scattering

$$S^{(W,\nu)} = -\frac{1}{(2\pi)^8}\sum_{n',n}\sum_{s',s}\int d^3p' \int d^3p \int d^3k \frac{1}{4E'_\nu E_\nu}\delta(E'_n + E_\nu - E_n - E'_\nu)\int d^3x_1 \int d^3x_2 e^{-i(\mathbf{p}'+\mathbf{k})\cdot\mathbf{x}_1} e^{i(\mathbf{p}+\mathbf{k})\cdot\mathbf{x}_2}$$
$$\times \overline{u}^{(s')}(\mathbf{p}')V^\alpha \phi^{(+)}_n(\mathbf{x}_1) iD^W_{\alpha\beta}(k^0,\mathbf{k})\bar{\phi}^{(+)}_{n'}(\mathbf{x}_2)V^\beta u^{(s)}(\mathbf{p})N[b^\dagger_{s'}(\mathbf{p}')a_{n'}a^\dagger_n b_s(\mathbf{p})], \tag{A29}$$

where $k^0 = E_n - E_\nu$. The same substitutions into (A24) allows the integrations over d^4x_1, d^4k and dx_2^0 to be performed, resulting in the S-operator for Z-mediated ν_e scattering

$$S^{(Z,\nu)} = -\frac{1}{(2\pi)^5}\sum_{n',n}\sum_{s',s}\int d^3p' \int d^3p \frac{1}{4E'_\nu E_\nu}\delta(E'_n + E'_\nu - E_n - E_\nu)\int d^3x_2 e^{i(\mathbf{p}-\mathbf{p}')\cdot\mathbf{x}_2}$$
$$\times \bar{u}^{(s')}(\mathbf{p}')V^\alpha_\nu u^{(s)}(\mathbf{p}) iD^Z_{\alpha\beta}(p'-p)\bar{\phi}^{(+)}_{n'}(\mathbf{x}_2)V^\alpha_e \phi^{(+)}_n(\mathbf{x}_2)N[b^\dagger_{s'}(\mathbf{p}')b_s(\mathbf{p})a^\dagger_{n'}a_n]. \tag{A30}$$

Forming the S-matrix between the initial state

$$|i\rangle = b^\dagger_{s_i}(\mathbf{p}_{\nu_i})a^\dagger_{n_i}|\mathrm{Vac}\rangle \tag{A31}$$

and the final state

$$|f\rangle = b^\dagger_{s_f}(\mathbf{p}_{\nu_f})a^\dagger_{n_f}|\mathrm{Vac}\rangle \tag{A32}$$

gives

$$S^{(W,\nu)}_{fi} = -\frac{1}{(2\pi)^2}\delta(E^{(\nu)}_{fi})\int d^3k \int d^3x_1 \int d^3x_2 e^{-i(\mathbf{p}_{\nu_f}+\mathbf{k})\cdot\mathbf{x}_1} e^{i(\mathbf{p}_{\nu_i}+\mathbf{k})\cdot\mathbf{x}_2}$$
$$\times \bar{u}^{(s_f)}(\mathbf{p}_{\nu_f})V^\alpha \phi^{(+)}_{n_i}(\mathbf{x}_1) iD^W_{\alpha\beta}(k^0,\mathbf{k})\bar{\phi}^{(+)}_{n_f}(\mathbf{x}_2)V^\beta u^{(s_i)}(\mathbf{p}_{\nu_i}) \tag{A33}$$

and

$$S^{(Z,\nu)}_{fi} = -2\pi\delta(E^{(\nu)}_{fi})\int d^3x_2 e^{i(\mathbf{p}_{\nu_i}-\mathbf{p}_{\nu_f})\cdot\mathbf{x}_2}\bar{u}^{(s_f)}(\mathbf{p}_{\nu_f})V^\alpha_\nu u^{(s_i)}(\mathbf{p}_{\nu_i}) iD^Z_{\alpha\beta}(p_i - p_f)\bar{\phi}^{(+)}_{n_f}(\mathbf{x}_2)V^\alpha_e \phi^{(+)}_{n_i}(\mathbf{x}_2), \tag{A34}$$

where

$$\delta(E^{(\nu)}_{fi}) \equiv \delta(E_{n_f} + E_{\nu_f} - E_{n_i} - E_{\nu_i}). \tag{A35}$$

Since the scattering occurs at low momentum transfers $k^2 \ll M_A^2$, the gauge boson propagator, in the Feynman gauge $\xi = 1$, simplifies to

$$iD^A_{\alpha\beta}(k) = \frac{i}{M_A^2}g_{\alpha\beta}, \tag{A36}$$

and the integrations over d^3k and d^3x_1 in (A33) can now be performed. Noting that $M_W = M_Z\cos\theta_W$ and $g^2/(8M_W^2) = G_F/\sqrt{2}$, the S-matrix elements become

$$S_{fi}^{(W,\nu)} = -2\pi i \frac{G_F}{\sqrt{2}}\delta(E_{fi}^{(\nu)}) \int d^3x_2 e^{i(\mathbf{p}_{\nu_i}-\mathbf{p}_{\nu_f})\cdot\mathbf{x}_2} \times [\bar{u}^{(s_f)}(\mathbf{p}_{\nu_f})\gamma^\alpha(1-\gamma_5)\phi_{n_i}^{(+)}(\mathbf{x}_2)] \times [\bar{\phi}_{n_f}^{(+)}(\mathbf{x}_2)\gamma_\alpha(1-\gamma_5)u^{(s_i)}(\mathbf{p}_{\nu_i})], \tag{A37}$$

and

$$S_{fi}^{(Z,\nu)} = -\pi i \frac{G_F}{\sqrt{2}}\delta(E_{fi}^{(\nu)}) \int d^3x_2 e^{i(\mathbf{p}_{\nu_i}-\mathbf{p}_{\nu_f})\cdot\mathbf{x}_2} \times [\bar{u}^{(s_f)}(\mathbf{p}_{\nu_f})\gamma^\alpha(1-\gamma_5)u^{(s_i)}(\mathbf{p}_{\nu_i})] \times [\bar{\phi}_{n_f}^{(+)}(\mathbf{x}_2)\gamma_\alpha(v_e+a_e\gamma_5)\phi_{n_i}^{(+)}(\mathbf{x}_2)]. \tag{A38}$$

Using the Fierz transformation

$$[\bar{u}^{(s_f)}(\mathbf{p}_{\nu_f})\gamma^\alpha(1-\gamma_5)\phi_{n_i}^{(+)}(\mathbf{x}_2)] \times [\bar{\phi}_{n_f}^{(+)}(\mathbf{x}_2)\gamma_\alpha(v_e+a_e\gamma_5)u^{(s_i)}(\mathbf{p}_{\nu_i})] = [\bar{u}^{(s_f)}(\mathbf{p}_{\nu_f})\gamma^\alpha(1-\gamma_5)u^{(s_i)}(\mathbf{p}_{\nu_i})] \times [\bar{\phi}_{n_f}^{(+)}(\mathbf{x}_1)\gamma_\alpha(v_e+a_e\gamma_5)\phi_{n_i}^{(+)}(\mathbf{x}_1)] \tag{A39}$$

we can combine the S-matrices for W- and Z- mediated scattering to give the result (20).

APPENDIX B: EXPLICIT EXPRESSIONS FOR ELECTRON SCATTERING TENSORS

Explicit expressions for the electron scattering tensors $L^{\beta\alpha}_{v_e v_e}, L^{\beta\alpha}_{a_e a_e}, L^{\beta\alpha}_{v_e a_e}$, and $L^{\beta\alpha}_{a_e v_e}$ appearing in (65) are given here. For the case $(\alpha,\beta)=(0,0)$, we have

$$\begin{aligned}
L^{0,0}_{v_e v_e} &= I_{\bar{l}}^{gg*} I_l^{gg} \tilde{A}^{0,0}_{\bar{l}l}(l_f,l_i,l_f,l_i) + I_{\bar{l}}^{gg*} I_l^{ff} \tilde{A}^{0,0}_{\bar{l}l}(l_f,l_i,l'_f,l'_i) + I_{\bar{l}}^{ff*} I_l^{gg} \tilde{A}^{0,0}_{\bar{l}l}(l'_f,l'_i,l_f,l_i) + I_{\bar{l}}^{ff*} I_l^{ff} \tilde{A}^{0,0}_{\bar{l}l}(l'_f,l'_i,l'_f,l'_i),\\
L^{0,0}_{a_e a_e} &= I_{\bar{l}}^{gf*} I_l^{gf} \tilde{A}^{0,0}_{\bar{l}l}(l_f,l'_i,l_f,l'_i) - I_{\bar{l}}^{gf*} I_l^{fg} \tilde{A}^{0,0}_{\bar{l}l}(l_f,l'_i,l'_f,l_i) - I_{\bar{l}}^{fg*} I_l^{gf} \tilde{A}^{0,0}_{\bar{l}l}(l'_f,l_i,l_f,l'_i) + I_{\bar{l}}^{fg*} I_l^{fg} \tilde{A}^{0,0}_{\bar{l}l}(l'_f,l_i,l'_f,l_i),\\
L^{0,0}_{v_e a_e} &= i[I_{\bar{l}}^{gg*} I_l^{gf} \tilde{A}^{0,0}_{\bar{l}l}(l_f,l_i,l_f,l'_i) - I_{\bar{l}}^{gg*} I_l^{fg} \tilde{A}^{0,0}_{\bar{l}l}(l_f,l_i,l'_f,l_i) + I_{\bar{l}}^{ff*} I_l^{gf} \tilde{A}^{0,0}_{\bar{l}l}(l'_f,l'_i,l_f,l'_i) - I_{\bar{l}}^{ff*} I_l^{fg} \tilde{A}^{0,0}_{\bar{l}l}(l'_f,l'_i,l'_f,l_i)],\\
L^{0,0}_{a_e v_e} &= -i[I_{\bar{l}}^{gf*} I_l^{gg} \tilde{A}^{0,0}_{\bar{l}l}(l_f,l'_i,l_f,l_i) + I_{\bar{l}}^{gf*} I_l^{ff} \tilde{A}^{0,0}_{\bar{l}l}(l_f,l'_i,l'_f,l'_i) - I_{\bar{l}}^{fg*} I_l^{gg} \tilde{A}^{0,0}_{\bar{l}l}(l'_f,l_i,l_f,l_i) - I_{\bar{l}}^{fg*} I_l^{ff} \tilde{A}^{0,0}_{\bar{l}l}(l'_f,l_i,l'_f,l'_i)].
\end{aligned} \tag{B1}$$

The other cases can be obtained through the substitutions

$$\begin{aligned}
L^{k',k}_{v_e v_e} &= L^{0,0}_{a_e a_e}[\tilde{A}^{0,0}_{\bar{l}l}(l_1,l_2,l_3,l_4) \to \tilde{A}^{k',k}_{\bar{l}l}(l_1,l_2,l_3,l_4)]\\
L^{k',k}_{a_e a_e} &= L^{0,0}_{v_e v_e}[\tilde{A}^{0,0}_{\bar{l}l}(l_1,l_2,l_3,l_4) \to \tilde{A}^{k',k}_{\bar{l}l}(l_1,l_2,l_3,l_4)]\\
L^{k',k}_{v_e a_e} &= L^{0,0}_{v_e a_e}[\tilde{A}^{0,0}_{\bar{l}l}(l_1,l_2,l_3,l_4) \to \tilde{A}^{k',k}_{\bar{l}l}(l_1,l_2,l_3,l_4)]\\
L^{k',k}_{a_e v_e} &= L^{0,0}_{a_e v_e}[\tilde{A}^{0,0}_{\bar{l}l}(l_1,l_2,l_3,l_4) \to \tilde{A}^{k',k}_{\bar{l}l}(l_1,l_2,l_3,l_4)]\\
L^{0,k}_{v_e v_e} &= L^{0,0}_{v_e a_e}[\tilde{A}^{0,0}_{\bar{l}l}(l_1,l_2,l_3,l_4) \to \tilde{A}^{0,k}_{\bar{l}l}(l_1,l_2,l_3,l_4)]\\
L^{0,k}_{a_e a_e} &= L^{0,0}_{a_e v_e}[\tilde{A}^{0,0}_{\bar{l}l}(l_1,l_2,l_3,l_4) \to \tilde{A}^{0,k}_{\bar{l}l}(l_1,l_2,l_3,l_4)]\\
L^{0,k}_{v_e a_e} &= L^{0,0}_{v_e v_e}[\tilde{A}^{0,0}_{\bar{l}l}(l_1,l_2,l_3,l_4) \to \tilde{A}^{0,k}_{\bar{l}l}(l_1,l_2,l_3,l_4)]\\
L^{0,k}_{a_e v_e} &= L^{0,0}_{a_e a_e}[\tilde{A}^{0,0}_{\bar{l}l}(l_1,l_2,l_3,l_4) \to \tilde{A}^{0,k}_{\bar{l}l}(l_1,l_2,l_3,l_4)].
\end{aligned} \tag{B2}$$

Using the symmetry

$$A_{ll}^{(I,I)}(l_1,l_2,l_3,l_4) = A_{ll}^{(I,I)}(l_3,l_4,l_1,l_2), \tag{B3}$$

and noting that the radial integrals are real, then

$$L^{0,0}_{v_e a_e} = L^{0,0}_{a_e v_e}, \tag{B4}$$

and these terms cancel in (65). Similarly, the symmetry

$$A_{\bar{l}l}^{(\lambda,\lambda)}(l_1,l_2,l_3,l_4) = (-1)^{l+\bar{l}} A_{\bar{l}l}^{(-\lambda,-\lambda)}(l_3,l_4,l_1,l_2), \tag{B5}$$

gives

$$L^{k,k}_{v_e a_e} = L^{k,k}_{a_e v_e} = 0. \tag{B6}$$

Hence all the diagonal elements of $L_{fi}^{(e)}(\tilde{\mathbf{q}})^{\beta\alpha}$ are real.

APPENDIX C: EVALUATION OF RADIAL MATRIX ELEMENTS

The evaluation of the radial matrix elements (45) requires the integration of the radial Dirac equations (38) to obtain the continuum eigenfunction

$$y_{\kappa_f,E_f}(r) \equiv \begin{pmatrix} g_{\kappa_f,E_f}(r) \\ f_{\kappa_f,E_f}(r) \end{pmatrix}, \tag{C1}$$

and the subsequent integration over a product of the initial bound state eigenfunction (71), this continuum eigenfunction, and the spherical Bessel function $j_l(qr)$.

The continuum eigenfunctions are regular at the origin and asymptotic to standing waves. These solutions increase as r^{γ_f} until the point $r_s \approx |\kappa_f|/p$ where they become oscillatory with approximately constant amplitude. As γ_f can be quite large, the smoothed functions [30,31]

$$\mathcal{Y}_{\kappa_f,E_f}(r) \equiv r^{-\gamma_f} y_{\kappa_f,E_f}(r), \tag{C2}$$

are integrated outwards from $r = 0$ until the first maximum or minimum of $\mathcal{Y}_{\kappa_f,E_f}(r)$ is reached. These smoothed solutions satisfy

$$\frac{d\mathcal{Y}_{\kappa_f,E_f}(r)}{dr} = a(r,\gamma_f)\mathcal{Y}_{\kappa_f,E_f}(r), \tag{C3}$$

where

$$a(r,\gamma_f) = \begin{pmatrix} -(\kappa_f+\gamma_f)/r & E_f+m_e-V(r) \\ -(E_f-m_e-V(r)) & (\kappa_f-\gamma_f)/r \end{pmatrix}. \tag{C4}$$

The starting values were obtained from a series expansion about the origin

$$\mathcal{Y}_{\kappa_f,E_f}(r) = \sum_{n=0} \begin{pmatrix} a_n \\ b_n \end{pmatrix} r^n, \tag{C5}$$

where the coefficients a_n and b_n $(n \geq 1)$ satisfy the recurrence relations

$$\begin{aligned} a_n &= [\alpha Z(m_e - E_f)a_{n-1} \\ &\quad + (m_e + E_f)(n + \gamma_f - \kappa_f)b_{n-1}]/n(2\gamma_f + n), \\ b_n &= -[\alpha Z(m_e + E_f)b_{n-1} \\ &\quad + (E_f - m_e)(n + \gamma_f + \kappa_f)a_{n-1}]/n(2\gamma_f + n), \end{aligned} \tag{C6}$$

with a_0 and b_0 determined from

$$b_0 = \left(\frac{\alpha Z}{\kappa_f - \gamma_f}\right) a_0, \qquad (\kappa_f < 0), \tag{C7}$$

and

$$a_0 = \left(\frac{\alpha Z}{\kappa_f + \gamma_f}\right) b_0, \qquad (\kappa_f > 0). \tag{C8}$$

As the differential equations (C3) are linear, the values $a_0 = 1$ $(\kappa_f < 0)$ and $b_0 = 1$ $(\kappa_f > 0)$ may be used as initial conditions. However, the energy normalization condition

$$\int_0^\infty (g^*_{\kappa'_f E'_f} g_{\kappa_f E_f} + f^*_{\kappa'_f E'_f} f_{\kappa_f E_f}) dr = \delta_{\kappa'_f,\kappa_f} m_e \delta(E'_f - E_f) \tag{C9}$$

requires that the computed solutions be corrected by the factors [31]

$$a_0 = 2N_f \sqrt{E_f + m_e}(2p_f)^{\gamma_f}\{\gamma_f \cos\eta - y \sin\eta\}, \tag{C10}$$

for $\kappa_f < 0$, and

$$b_0 = -2N_f \sqrt{E_f - m_e}(2p_f)^{\gamma_f}\{\gamma_f \sin\eta + y \cos\eta\}, \tag{C11}$$

for $\kappa_f > 0$.

The differential equations (C3) were integrated using a fifth-order Runge-Kutta method [32]. The rapid propagation of initial errors that arises from the r^{-1} term in $a(r,\gamma_f)$ was controlled by the use of the series expansion for the first $5|\kappa_f|$ points of the integration mesh [31]. The integration algorithm correctly reproduced the free field solutions (87) for $Z = 0$ and the asymptotic forms

$$\begin{pmatrix} g_{\kappa_f,E_f}(r) \\ f_{\kappa_f,E_f}(r) \end{pmatrix} = \sqrt{\frac{m_e}{\pi p_f}} \begin{pmatrix} \sqrt{E_f + m_e}\cos(p_f r + \delta_f) \\ -\sqrt{E_f - m_e}\sin(p_f r + \delta_f) \end{pmatrix}, \tag{C12}$$

for $Z \neq 0$, where the Coulombic phase is [23]

$$\delta_f = y_f \log(2p_f r) - \arg[\Gamma(\gamma_f + iy_f)] + \eta_f - \pi\gamma_f/2. \tag{C13}$$

The radial integrals (45) have the form

$$\mathcal{I}_l(q) = \int_0^\infty (\lambda_i r)^{\gamma_i+\beta_i} e^{-\lambda_i r} j_l(qr) y_{\kappa_f,E_f}(r) dr, \tag{C14}$$

where $\beta_i = 0$, 1, and were evaluated using an upper limit $r_\infty = x_\infty/\lambda_i$ with x_∞ chosen to ensure $rj_l(qr)$ and $y_{\kappa_f,E_f}(r)$ had attained their oscillatory forms. This required the condition

$$r_\infty > \max\left(\frac{\sqrt{l(l+1)}}{q}, \frac{\sqrt{l_f(l_f+1)}}{p_f}, \frac{\sqrt{l'_f(l'_f+1)}}{p_f}\right) \tag{C15}$$

to be satisfied. Since $q_{\min} = \epsilon_f + \epsilon_i$, then, for ϵ_f in the range [11] (0.01–5.0) keV, the smallest value of $q_{\min}$ occurs for H and is 4.6×10^{-5}. Since $p_f \approx \sqrt{2\epsilon_f}$ for small ϵ_f, then $p_{f,\min} \sim 6.3 \times 10^{-3}$. Thus the condition on $j_l(qr)$ is the most challenging to meet.

[1] J. D. Vergados and Yu. N. Novikov, Exploring new features of neutrino oscillations with very low energy monoenergetic neutrinos, Nucl. Phys. **B839**, 1 (2010).

[2] A. W. Thomas and J. D. Vergados, Solar neutrinos as background in dark matter searches involving electron detection, J. Phys. G **43**, 07LT01 (2016).

[3] M. D. Campos and W. Rodejohann, Testing keV sterile neutrino dark matter in future direct detection experiments, Phys. Rev. D **94**, 095010 (2016).

[4] C. Giunti and A. Studenikin, Neutrino electromagnetic interactions: A window to new physics, Rev. Mod. Phys. **87**, 531 (2015).

[5] J. Jeong, J. E. Kim, and S. Youn, Electromagnetic properties of neutrinos from scattering on bound electrons in atoms, Int. J. Mod. Phys. A **36**, 2150182 (2021).

[6] K. A. Kouzakov and A. I. Studenikin, Theory of neutrino-atom collisions: The history, present status, and BSM physics, Adv. High Energy Phys. **2014**, 1 (2014).

[7] Yu. V. Gaponov, Yu. L. Doprynin, and V. I. Tikhonov, Elastic scattering of low energy neutrinos by atomic systems, Sov. J. Nucl. Phys. **22**, 170 (1975).

[8] S. A. Fayans, V. Yu. Dobretsov, and A. B. Dobrotsvetov, Effect of atomic binding on inelastic νe scattering, Phys. Lett. B **291**, 1 (1992).

[9] V. Yu. Dobretsov, A. B. Dobrotsvetov, and S. A. Fayans, Inelastic neutrino scattering by atomic electrons, Sov. J. Nucl. Phys. **55**, 1180 (1992).

[10] G. J. Gounaris, E. A. Paschos, and P. I. Porfyriadis, The ionization of H, He or Ne atoms using neutrinos or antineutrinos at keV energies, Phys. Lett. B **525**, 63 (2002).

[11] G. J. Gounaris, E. A. Paschos, and P. I. Porfyriadis, Electron spectra in the ionization of atoms by neutrinos, Phys. Rev. D **70**, 113008 (2004).

[12] M. B. Voloshin, Neutrino Scattering on Atomic Electrons in Searches for the Neutrino Magnetic Moment, Phys. Rev. Lett. **105**, 201801 (2010).

[13] K. A. Kouzakov and A. I. Studenikin, Magnetic neutrino scattering on atomic electrons revisited, Phys. Lett. B **696**, 252 (2011).

[14] K. A. Kouzakov, A. I. Studenikin, and M. B. Voloshin, Neutrino-impact ionization of atoms in searches for neutrino magnetic moment, Phys. Rev. D **83**, 113001 (2011).

[15] J.-W. Chen, C.-P. Liu, C.-L. Wu, and C.-P. Wu, Ionization of hydrogen by neutrino magnetic moment, relativistic muon, and WIMP, Phys. Rev. D **88**, 033006 (2013).

[16] J.-W. Chen, H.-C. Chi, K.-N. Huang, C.-P. Liu, H.-T. Shiao, L. Singh, H. T. Wong, C.-L. Wu, and C.-P. Wu, Atomic ionization of germanium by neutrinos from *ab initio* approach, Phys. Lett. B **731**, 159 (2014).

[17] J.-W. Chen, H.-C. Chi, K.-N. Huang, H. Bin Li, C.-P. Liu, L. Singh, H. T. Wong, C.-L. Wu, and C.-P. Wu, Constraining neutrino electromagnetic properties by germanium detectors, Phys. Rev. D **91**, 013005 (2015).

[18] I. B. Whittingham, Incoherent scattering of gamma rays in heavy atoms, J. Phys. A **4**, 21 (1971).

[19] W. H. Furry, On bound states and scattering in positron theory, Phys. Rev. **81**, 115 (1951).

[20] C. Itzykson and J. B. Zuber, *Quantum Field Theory* (McGraw-Hill, New York, 1980).

[21] D. Bailin, *Weak Interactions*, 2nd ed. (Adam Hilger, Bristol, 1982).

[22] J. M. Jauch and F. Rohrlich, *The Theory of Photons and Electrons* (Addison-Wesley, Reading, 1955).

[23] M. E. Rose, *Relativistic Electron Theory* (Wiley, New York, 1961).

[24] H. Olsen, Outgoing and ingoing waves in final states and bremsstrahlung, Phys. Rev. **99**, 1335 (1955).

[25] M. E. Rose, *Elementary Theory of Angular Momentum* (Wiley, New York, 1957).

[26] H. A. Bethe and E. E. Salpeter, *Quantum Mechanics of One- and Two- Electron Atoms* (Springer-Verlag, Berlin, 1957).

[27] D. Thomas, https://www.uoguelph.ca/chemistry/thomas/index.

[28] J. H. Schofield, Theoretical photoionization cross sections from 1 to 1500 keV, Lawrence Livermore Laboratory report UCRL-51326 (1973), 10.2172/4545040.

[29] J. Wimp, *Sequence Transformations and Their Applications*, (Academic Press, New York, 1981), p. 169.

[30] R. H. Pratt, R. D. Levee, R. L. Paxton, and W. Aron, *K*-shell photoelectric cross sections from 200 keV to 2 MeV, Phys. Rev. **134**, A898 (1964).

[31] W. R. Johnson, Angular distribution of single-quantum annihilation radiation, Phys. Rev. **159**, 61 (1967).

[32] W. H. Press, S. A. Teukolsky, W. T. Vetterling, and B. P. Flannery, *Numerical Recipes in Fortran*, 2nd ed. (Cambridge University Press, Cambridge, England, 1992).